

Mutual Regulation of Epicardial Adipose Tissue and Myocardial Redox State by PPAR- γ /Adiponectin Signalling

Alexios S. Antonopoulos^{a*}, Marios Margaritis^{a*}, Sander Verheule^b, Alice Recalde^a, Fabio Sanna^a, Laura Herdman^a, Costas Psarros^a, Hussein Nasrallah^b, Patricia Coutinho^a, Ioannis Akoumianakis^a, Alison C. Brewer^d, Rana Sayeed^e, George Krasopoulos^e, Mario Petrou^e, Akansha Tarun^a, Dimitris Tousoulis^c, Ajay M. Shah^d, Barbara Casadei^a, Keith M. Channon^a, Charalambos Antoniades^a

^aDivision of Cardiovascular Medicine, Radcliffe Department of Medicine, University of Oxford, United Kingdom

^bCardiac Electrophysiology Group, Department of Physiology, Maastricht University, Netherlands

^cDepartment of Cardiology, Athens University Medical School, Athens, Greece

^dCardiovascular Division, King's College London BHF Centre, London, United Kingdom

^eDepartment of Cardiac Surgery, John Radcliffe Hospital, Oxford United Kingdom

1st Author's Surname Antonopoulos

Short title: Epicardial adipose tissue and myocardial redox

Word count (text, figure legends, table, references): 8,681; **References:** 43; **Figures:** 7

Subject Codes: [7] Chronic ischemic heart disease, [91] Oxidant stress

*Authors equally contributed to the study

Supplementary files: 1

Corresponding author

Charalambos Antoniades MD PhD

Associate Professor of Cardiovascular Medicine

Division of Cardiovascular Medicine, University of Oxford

John Radcliffe Hospital, Oxford OX3 9DU, United Kingdom

Tel: +44-1865-221870, Fax: +44-1865-740352

e-mail: antoniad@well.ox.ac.uk

Abstract

Rationale: Adiponectin has anti-inflammatory effects in experimental models but its role in the regulation of myocardial redox state in humans is unknown. Although adiponectin is released from epicardial adipose tissue (EpAT), it is unclear whether it exerts any paracrine effects on the human myocardium.

Objective: To explore the cross-talk between EpAT-derived adiponectin and myocardial redox state in the human heart.

Methods and Results: EpAT and atrial myocardium were obtained from 306 patients undergoing CABG. Functional genetic polymorphisms that increase *ADIPOQ* expression (encoding adiponectin) led to reduced myocardial NADPH oxidase-derived $O_2^{\cdot-}$, whereas circulating adiponectin and *ADIPOQ* expression in EpAT were associated with elevated myocardial $O_2^{\cdot-}$. In human atrial tissue, we demonstrated that adiponectin suppresses myocardial NADPH oxidase activity, by preventing AMP kinase-mediated translocation of Rac1 and p47^{phox} from the cytosol to the membranes. Induction of $O_2^{\cdot-}$ production in H9C2 cardiomyocytes led to the release of a transferable factor able to induce PPAR- γ mediated up-regulation of *ADIPOQ* expression in co-cultured EpAT. Using a *NOX2* transgenic mouse and a pig model of rapid atrial pacing, we found that oxidation products (such as 4-hydroxynonenal) released from the heart trigger PPAR- γ mediated up-regulation of *ADIPOQ* in EpAT.

Conclusions: We demonstrate for the first time in humans, that adiponectin directly decreases myocardial NADPH oxidase activity via endocrine or paracrine effects. Adiponectin expression in EpAT is controlled by paracrine effects of oxidation products released from the heart. These effects constitute a novel defence mechanism of the heart against myocardial oxidative stress.

Key words: epicardial adipose tissue; adiponectin; NADPH oxidases; obesity; myocardium

Non-Standard Abbreviations and Acronyms

4HNE: 4-hydroxynonenal
ACC: acetyl-coA carboxylase
AMPK: AMP-kinase
BNP: Brain natriuretic peptide
CABG: coronary artery bypass grafting
CC: Compound C
CRP: C-reactive protein
EpAT: epicardial adipose tissue
GTP: Guanosine-5'-triphosphate
IHD: ischemic heart disease
MDA: malonyldialdehyde
PMA: Phorbol-12-Myristate-13-Acetate
PKC- α : protein kinase C- α
PPAR: peroxisome proliferator-activated receptor
qRT-PCR: Quantitative Real Time-Polymerase Chain Reaction
ThAT: thoracic adipose tissue

Dysregulation of myocardial redox signalling is involved in the pathophysiology of multiple cardiac diseases.¹ NADPH-oxidases are major enzymatic sources of reactive oxygen species in the heart² and have been linked in the past to cardiac pathologies such as atrial fibrillation,³⁻⁵ myocardial hypertrophy,⁶ heart failure,⁷ and others.⁸ Metabolic abnormalities such as obesity or diabetes are associated with increased NADPH oxidases activity in the cardiovascular system,^{8, 9} although the underlying mechanisms of these links are controversial.^{10, 11} Since pharmacological treatments able to suppress myocardial NADPH-oxidases (e.g. statins as part of their pleiotropic effects in the human heart⁵) have failed to prevent cardiac disease progression in humans,¹² better understanding of the endogenous mechanisms regulating NADPH oxidases in the human heart is essential for the development of new therapeutic strategies to target myocardial redox state.¹³

Adipose tissue affects the cardiovascular system by secreting a wide range of bioactive products known as adipokines.¹⁴ Adiponectin is an important adipokine with anti-inflammatory¹⁵ and antioxidant effects on the vasculature¹⁶ and the heart of experimental models,¹⁷ but its role in the regulation of myocardial redox state in humans is unknown.

In healthy individuals, low circulating adiponectin is associated with increased cardiovascular risk,¹⁸ however in individuals with ischemic heart disease (IHD) adiponectin gene expression in adipose tissue is increased¹⁹ and high circulating adiponectin predicts adverse clinical outcome.²⁰ Importantly, given that the human heart is surrounded by biologically active epicardial adipose tissue (EpAT), adiponectin released from it may exert additional paracrine effects on the underlying myocardium in a similar way perivascular adipose tissue exerts paracrine effects on the vascular wall,²¹ a concept that has not been previously explored.

In this study, we explore the role of adiponectin in the regulation of myocardial redox state in patients with IHD, and we characterize the underlying molecular mechanisms mediating adiponectin's effects on the heart. In addition, we define the mechanisms controlling peroxisome proliferator-activated receptor (PPAR)- γ /adiponectin signalling in human EpAT, and we introduce the novel concept of an "inside to outside" signalling released from the human heart in conditions of increased myocardial oxidative stress which controls the biosynthetic activity of the neighbouring EpAT.

Methods

Study Population

The study population consisted of 306 patients undergoing coronary artery bypass grafting surgery (CABG); 247 of these were included in the Clinical Associations Studies and 59 into the *ex vivo* arm of the study. Blood samples were obtained on the morning of surgery, while samples of myocardium and adipose tissue were collected during surgery, as described below. Myocardial and adipose tissue samples were used for *ex vivo* experiments to address the mechanisms regulating the crosstalk between EpAT and human myocardium as described below. Exclusion criteria were any inflammatory, infectious, liver or renal disease or malignancy. Patients receiving non-steroidal anti-inflammatory drugs, dietary supplements, or antioxidant vitamins were also excluded.

Design of the Clinical Associations Studies

In 247 patients undergoing CABG, blood samples were collected at the morning of surgery for measuring circulating adiponectin and other biomarkers as well as for DNA extraction and genotyping. Samples of right atrial appendage obtained from the cannulation site,⁵ were used to quantify NADPH-oxidases-derived superoxide anions ($O_2^{\cdot-}$) aiming to relate it with circulating adiponectin as well as the expression of *ADIPOQ* gene (encoding adiponectin) in different adipose tissue depots. These myocardial samples were also used to study the myocardial expression of *ADIPOQ* and adiponectin receptors. In addition, EpAT from the atrioventricular groove and thoracic adipose tissue (ThAT) from the outer surface of the pericardium¹⁹ were collected and used to quantify the expression of *ADIPOQ* and other target genes, aiming to search for predictors of myocardial redox state as described below. More detail on samples collection and processing is provided in the online Supplement.

Blood Sampling and Measurement of Circulating Biomarkers

Venous blood samples were obtained after 8 hours of fasting, on the morning of the operation, and used for measurement of circulating biomarkers (as described in the online Supplement).

DNA Extraction and Genotyping

Genomic DNA extraction from whole blood and genotyping were performed using standard methods (as described in the online Supplement).

Myocardial Superoxide Measurements

Myocardial $O_2^{\cdot-}$ production was measured in right atrial appendage samples using lucigenin (5 $\mu\text{mol/L}$)-enhanced chemiluminescence (as described in the online Supplement).

RNA Isolation and Quantitative Real Time-Polymerase Chain Reaction (qRT-PCR)

Samples of adipose tissue and right atrial appendage were used for RNA extraction and gene expression studies (as described in the online Supplement).

Ex Vivo Experiments With Human Myocardium

To examine the direct effects of adiponectin on myocardial $O_2^{\cdot-}$ production, human myocardial tissue from the right atrial appendage was incubated *ex vivo* for 2 hours with/without adiponectin in the presence/absence of the pharmacologic inhibitor of AMP-kinase (AMPK), Compound C (CC). Briefly, myocardial tissue was washed in ice-cold Krebs HEPES buffer and then cut into thin strips containing all myocardial layers. The tissue was first equilibrated for 20min in Krebs HEPES Buffer pH 7.35 at 37°C and then incubated for 2 hours in the presence or absence of recombinant full-length adiponectin 0.3 $\mu\text{mol/L}$ (10 $\mu\text{g/ml}$, BioVendor) +/- CC (10 $\mu\text{mol/L}$). The effect of adiponectin on myocardial $O_2^{\cdot-}$ (basal and NADPH-stimulated $O_2^{\cdot-}$) was quantified by lucigenin (5 $\mu\text{mol/L}$) enhanced chemiluminescence (as described in the online Supplement). To estimate the effect of adiponectin on NADPH-oxidase derived $O_2^{\cdot-}$, we used the pan-NADPH oxidase inhibitor Vas2870²² (40 $\mu\text{mol/L}$, Sigma Aldrich).

Ex Vivo Experiments with Human Adipose Tissue

Samples of ThAT and EpAT obtained from patients in the *ex vivo* study arm were used to estimate the effects of lipid oxidation products on *ADIPOQ* gene expression in an *ex vivo* bioassay. Briefly, adipose tissue was isolated and washed in sterile phosphate buffer saline (PBS). The samples of adipose tissue of each type were transferred to the laboratory within 30 minutes of harvesting. The samples were then cut into ~1-2 mm³ cubes, washed, and equilibrated for 2 hours at 37°C in Medium-199 containing HEPES (25 mmol/L), gentamycin 105 $\mu\text{mol/L}$ (50 $\mu\text{g/ml}$), and fatty acid-free bovine serum albumin (1%), in the presence of protease inhibitor (Roche Applied Science) in a cell culture incubator with 5% CO₂ atmosphere. At the end of the equilibration period, the media was replaced by fresh media (1ml per 200mg tissue) and incubated for 16 hours as above but in the presence or absence of (1) H₂O₂ (100 $\mu\text{mol/L}$), (2) malonyldialdehyde (MDA, 1mmol/L), (3) 4-hydroxynonenal (HNE, 30 $\mu\text{mol/L}$) +/- T0070907 (10 $\mu\text{mol/L}$, an inhibitor of PPAR- γ). For the samples treated with T0070907, this agent was also used during the equilibration period. At the end of the 16 hour incubation period, AT samples were filtered, collected, and stored at -80°C until analysis. qRT-PCRs were performed (as described in the online Supplement) to determine *ADIPOQ*, *PPAR- γ* and *CD36* gene expression.

Co-cultures of Rat Epicardial Adipose Tissue with H9c2 Cells

To evaluate the interaction between AT and myocardium, the rat cardiomyocyte-derived cell line H9c2 was co-incubated with rat EpAT *ex vivo*. Briefly, H9c2 cells were differentiated to cardiomyocytes in Dulbecco's Modified Eagle Medium (Sigma-Aldrich) supplemented with 1% horse serum (Sigma-Aldrich). The cells were exposed to either NADPH (100 $\mu\text{mol/L}$) or phorbol-12-Myristate-13-Acetate (PMA, 160nmol/L) for 2 hours as a means to induce $O_2^{\cdot-}$ generation from NADPH oxidases. Freshly collected rat EpAT from female Wistar rats was then added to the culture medium and co-incubated with H9c2-derived cardiomyocytes with or without NADPH (100 $\mu\text{mol/L}$ n=7) or PMA 160nmol/L (n=7) for 16 hours. To control for direct effects of NADPH or PMA on adipose tissue, EpAT was also incubated alone in the presence or absence of NADPH (100 $\mu\text{mol/L}$) or PMA (160nmol/L). To prevent any direct effects of endogenous $O_2^{\cdot-}$ in EpAT, additional interventions with NADPH (100 $\mu\text{mol/L}$) and PEG-SOD (300U/ml, a scavenger of $O_2^{\cdot-}$) or Vas2870 (10 nmol/L, an inhibitor of NADPH oxidases) were included. At the end of the incubation period, EpAT was collected for gene expression studies (as described in the online Supplement).

Measurement of intracellular NADP/NADPH levels

Intracellular NADP/NADPH levels were measured using a commercially available fluorometric assay (Abcam kit, Cambridge, UK) as described in the online Supplement.

Western Blots in Human Myocardial Samples

Western blotting was performed as described in the online Supplement.

Measurement of Myocardial Rac1 Activation and Membrane Translocation Experiments

Rac1 activation and membrane translocation of Rac1 and p47^{phox} were determined in right atrial appendage samples, as previously described²³ (online Supplement).

Animal studies

Mouse model: Cardiomyocyte-specific *NOX2*-transgenic mice²⁴ (*mNOX2-tg*, see online Supplement) were used as a model of chronically increased myocardial oxidative stress to test the impact of increased myocardial Nox2-derived O₂^{•-} production on adiponectin expression in subcutaneous and pericardial adipose tissue (attached to the apex of the heart).

Male 20-week old transgenic mice and wild-type littermate controls were sacrificed and whole heart samples as well as samples of subcutaneous and pericardial AT were harvested and studied.

Pig model: Given the limitations related to the study of pericardial AT in mice (limited amount of tissue, not always present), we used a larger mammal model (pig), whose EpAT is directly attached on the heart muscle, mimicking the interaction between myocardium and EpAT in humans. To induce a chronic increase in oxidative stress in the atrial myocardium⁴ we used a standardized protocol of rapid atrial pacing for 4 weeks and collected EpAT from the posterior left atrium at the end of this period. Subcutaneous AT was used as a control depot. More details on the pig model are provided in the online Supplement.

Myocardial tissue samples from the two animal models were homogenised and used for lucigenin-enhanced chemiluminescence experiments to assess myocardial NADPH-oxidases activity (as described in the online Supplement) and to blot for 4HNE and MDA protein adducts (antibodies by Abcam). RNA was extracted from myocardial and AT samples and used for gene expression studies (as described in the online Supplement).

Statistical Analysis

Continuous variables were tested for normal distribution using Kolmogorov-Smirnov test. Non-normally distributed variables were log-transformed for analysis. In the Clinical Associations Study arm, continuous variables among 3 groups were compared by use of 1-way ANOVA followed by the Bonferroni post hoc test for individual comparisons, whereas comparisons between 2 groups were performed by unpaired t-tests. Categorical variables were compared by use of the χ^2 test as appropriate. Correlations between continuous variables were assessed by bivariate analysis, and the Pearson coefficient was estimated.

For the ex vivo experiments (in which serial segments from the same right atrial appendage were incubated with multiple interventions), we performed repeated-measures ANOVA and paired t-tests for individual comparisons, followed by the Bonferroni post hoc correction for multiple testing as appropriate. In the Clinical Associations study arm, correlations between continuous variables were tested by calculating the Pearson correlation coefficient. Multivariable linear regression was performed by using log(NADPH-stimulated O₂^{•-}) or log(serum adiponectin) as dependent variables and by using demographic/biological variables that showed a significant association with the dependent variable in univariate analysis at the level of 15% as independent variables.

For the animal studies, comparisons of *mNOX2-tg* vs wild type mice or rapid atrial pacing vs sham were performed using unpaired t-test of the log-transformed values for the respective variables. Power calculations are provided in the data supplement. All statistical tests were performed with SPSS version 20.0 and values of $P < 0.05$ were considered statistically significant.

Results

Interactions Between Adiponectin and Myocardial NADPH Oxidases Activity in Patients with Ischaemic Heart Disease

The characteristics of the patients included in the Clinical Associations Studies are presented in Table 1. In this cohort of patients with ischaemic heart disease, we first explored the association between adiponectin levels and myocardial redox state. We observed a positive association between circulating adiponectin and myocardial NADPH-stimulated $O_2^{\cdot-}$ (Figure 1A), as well as between circulating adiponectin and MDA (Figure 1B), a plasma marker of oxidative stress. However, there was no significant association between adiponectin and either interleukin-6 (IL-6, Figure 1C) or high sensitivity C-reactive protein (hs-CRP, Figure 1D), suggesting that systemic inflammation does not confound the association between circulating adiponectin and myocardial NADPH oxidases activity. We also observed a significant association between plasma Brain Natriuretic Peptide (BNP) and circulating adiponectin (Figure 1E), but not between BNP and NADPH-stimulated $O_2^{\cdot-}$ in the myocardium (Online Table I) or plasma MDA ($r=0.147$, $P=0.092$). To further explore the association between myocardial redox state and serum adiponectin, we performed univariate analysis followed by multivariable analysis searching for predictors of myocardial NADPH oxidases-derived $O_2^{\cdot-}$ (Online Table I), confirming that the correlation between circulating adiponectin and myocardial NADPH-oxidases activity is independent of BNP and other potential confounders (Figure 1A, Online Table I). In addition, this was independent of medication such as statins ($\beta_{st}=-0.314$, $P=0.0001$), antiplatelet treatment ($\beta_{st}=-0.179$, $P=0.29$), beta blockers ($\beta_{st}=0.013$, $P=0.877$), calcium channel blockers ($\beta_{st}=-0.019$, $P=0.807$), or ACEi/ARB ($\beta_{st}=0.016$, $P=0.833$), with R^2 for the model 0.238. Interestingly, serum levels of adiponectin or *ADIPOQ* gene expression in EpAT were not related with the incidence of post-operative atrial fibrillation (data not shown), which we have previously shown to be increased in patients with high atrial NADPH-oxidases activity.⁵

To further explore the association between adiponectin and myocardial redox state, we genotyped our study population for two functional SNPs in the *ADIPOQ* locus encoding adiponectin (both SNPs with known effect on adiponectin levels), located in the *ADIPOQ* locus (rs266717) and in the promoter region (rs17366568).^{25, 26} We found that the number of rs266717G and rs17366568T alleles was positively associated with serum adiponectin (Figure 2A) and negatively associated with myocardial NADPH-oxidases activity (Figure 2B). This implies that low adiponectin production in human AT is causally associated with higher myocardial NADPH-oxidases activity. Furthermore, there was a significant effect of the SNPs on the expression of *ADIPOQ* gene in ThAT (Figure 2C), but this was not observed in EpAT (Figure 2D), suggesting that local mechanisms may override the influence of genetic background on *ADIPOQ* gene expression in EpAT but not in “remote” adipose tissue depots such as ThAT.

We next examined whether obesity and adipose tissue distribution alter the regulation of *ADIPOQ* gene expression in different adipose tissue depots. We confirmed that *ADIPOQ* gene expression in ThAT was strongly inversely correlated with waist to hip ratio and BMI, while *PPAR-γ* expression was similarly correlated with waist to hip ratio (although its association with BMI was borderline significant, Online Figure I, Panels A to D). However, these associations were not present in EpAT (Online Figure I, Panels E to H). These discordant findings between EpAT and ThAT suggest that *PPAR-γ*/adiponectin signalling in EpAT is controlled by local mechanisms, possibly originating in the heart, rather than by systemic effects related to obesity and insulin resistance.

Importantly, there was a positive association between myocardial NADPH-stimulated $O_2^{\cdot-}$ and the expression of both *ADIPOQ* (Figure 2E) and *PPAR-γ* genes (Figure 2F) in EpAT, suggesting that increased myocardial $O_2^{\cdot-}$ may influence the expression of *ADIPOQ* in EpAT, possibly by regulating *PPAR-γ* expression. *ADIPOQ* gene expression is known to be partly under the control of *PPAR-γ* signalling. This was confirmed by the association between $\log(PPAR-γ)$ and $\log(ADIPOQ)$ gene expression in EpAT of patients with ischemic heart disease ($r=0.598$, $P<0.0001$).

To explore whether myocardial resistance to adiponectin is responsible for the positive association between myocardial redox state and adiponectin levels (systemic and EpAT expression), we studied the expression of *ADIPOQ* and adiponectin receptors (*ADIPOR1*, *ADIPOR2* and *CDH13*) in the myocardium of patients with advanced coronary atherosclerosis. There was no association between myocardial NADPH-oxidases activity and *ADIPOQ* gene expression (Figure 2G), while there was a positive association between myocardial NADPH-oxidase activity and *ADIPOR1* (but not *ADIPOR2* or *CDH13*, Figure 2H), suggesting that in the presence of increased myocardial ROS

generation, there is up-regulation of *ADIPOR1* in human myocardium as well as an up-regulation of *ADIPOQ* gene in EpAT.

Adiponectin Directly Decreases NADPH Oxidases Activity in the Human Myocardium

To examine whether adiponectin has the ability to affect myocardial redox state in humans, myocardial tissue from patients with ischaemic heart disease (Table 1) was incubated with adiponectin (10µg/ml) for 2 hours. Exogenous adiponectin rapidly induced phosphorylation of AMP-kinase (AMPK) at the activatory site Thr172 (Figure 3A) and the downstream target acetyl-coA carboxylase (ACC), via phosphorylation at Ser79 (Figure 3B). As expected the observed effects on ACC phosphorylation, a marker of AMPK activity, were prevented by the AMPK-inhibitor compound C (CC, Figure 3A-3B). Similarly, adiponectin induced a rapid reduction of myocardial $O_2^{\cdot -}$ production that was reversed by CC (Figure 3C). Importantly, adiponectin suppressed the Vas2870-inhibitable fraction of myocardial $O_2^{\cdot -}$ in a CC-inhibitable manner (Figure 3D), suggesting that adiponectin inhibits NADPH-oxidase activity via an AMPK-mediated mechanism. These AMPK-dependent effects of adiponectin were also confirmed in dihydroethidium staining experiments; adiponectin reduced both the total and the Vas2870-inhibitable dihydroethidium fluorescence (Figure 3E-3G). Adiponectin did not have any effects on the gene expression or protein levels of Nox isoforms or any NADPH oxidase subunits in human myocardium (Online Figure II), but prevented the activation of Rac1 (reduced the GTP-Rac1/total Rac1) and its membrane translocation (Figure 3H-3I), as well as the phosphorylation of the p47^{phox} subunit of Nox2 at its activatory site Ser359 and its membrane translocation (Figure 3J-3K). Both the effects of adiponectin on Rac1 and p47^{phox} were reversed by CC, suggesting that these effects involved AMPK signalling. Interestingly, the AMPK-mediated effects of adiponectin on Rac1 and p47^{phox} activation/membrane translocation were independent of any change in Akt activity, as evidenced by Western blotting for phospho-Akt at its activation site Ser473, or protein kinase C- α (PKC- α) phosphorylation status (Online Figure II).

These data suggest that adiponectin suppresses NADPH oxidases activity in the human myocardium in an AMPK-dependent mechanism. Taken together with the observed positive association between myocardial NADPH-oxidases activity and *ADIPOQ* gene expression in EpAT (Figure 2E), these findings suggest that myocardial $O_2^{\cdot -}$ production may be driving (directly or indirectly) the expression of PPAR- γ /*ADIPOQ* in EpAT.

Identifying a Novel, Redox Sensitive Signal from Cardiomyocytes to EpAT

To explore the hypothesis that the release of a transferable factor from cardiomyocytes under conditions of increased oxidative stress, may drive PPAR- γ /*ADIPOQ* expression in the EpAT, we exposed H9c2 cells to NADPH (100µmol/L, the substrate of NADPH-oxidases), for 2 hours (Figure 4A), as a means to increase the production of $O_2^{\cdot -}$ from NADPH-oxidases in these cells (Figure 4B and 4C). Exogenous NADPH increased intracellular NADPH by 25% (Online Figure III). The NADPH-simulated $O_2^{\cdot -}$ in these cells was inhibited by ~60% using pan-Nox inhibitor Vas2870 and by 50% using the specific Nox2 inhibitor gp91-dstat (Figure 4). At the end of the 2h incubation period with NADPH, we co-cultured freshly collected rat EpAT with the stimulated H9c2 cells for 16h (Figure 4A). At the end of the incubation period we measured gene expression in the EpAT from co-culture. There was no change in the expression of *ADIPOQ*, PPAR- γ , or *CD36* genes in rat EpAT incubated with NADPH alone or co-cultured with H9c2 cells without added NADPH (Figure 4D-4F). However, co-culture of rat EpAT with H9c2 cells pre-stimulated with NADPH resulted in a significant increase in *ADIPOQ* gene expression (Figure 4D) as well as expression of PPAR- γ (Figure 4E) and its downstream target *CD36* (Figure 4F). These effects were all prevented by the $O_2^{\cdot -}$ scavenger PEG-SOD or the NADPH oxidases inhibitor Vas2870 (Figure 4D-4F). These findings indicate that increased $O_2^{\cdot -}$ production from H9c2 cells leads (either directly or indirectly via an intermediate factor) to up-regulation of PPAR- γ /adiponectin expression in rat EpAT.

As an alternative model to stimulate $O_2^{\cdot -}$ generation in H9C2 cells in the above experiment, we repeated the same experimental design by using PMA 160nmol/L instead of NADPH (Online Figure IV). We observed a similar up-regulation of *ADIPOQ* and *PPAR-γ* in rat EpAT that was inhibitable by Vas2870. However, the same effect was also observed in the absence of H9C2 cells, suggesting a direct effect of PMA on *PPAR-γ* signaling in the EpAT (Online Figure IV).

Myocardial Oxidation Products as Candidate Mediators of Inside-to-Outside Cardiac-Adipose Tissue Signalling

Since $O_2^{\cdot -}$ is a short-lived, highly reactive molecule, we hypothesised that other longer-lived reactive oxygen species rather than $O_2^{\cdot -}$ itself (e.g. H_2O_2) or even products of lipid oxidation could act as transferable factors released from cardiomyocytes under oxidative stress conditions to exert a paracrine effect on EpAT. Incubation of human EpAT with H_2O_2 (100μmol/L) suppressed *ADIPOQ* gene expression (Online Figure VI, Panel A), suggesting that direct exposure of EpAT to H_2O_2 cannot explain the observation in the Clinical Associations Studies that high myocardial oxidative stress is linked to high *ADIPOQ* expression in EpAT (Figure 2E).

Next we examined whether products of lipid oxidation (formed under conditions of high myocardial oxidative stress) could modulate *ADIPOQ* expression in EpAT. We found that increased activity of NADPH-oxidases in the human myocardium leads to increased formation of common oxidation products, such as 4HNE and MDA, which form detectable adducts with proteins in the human myocardium (Figure 5A-5B). 4HNE adducts are also rapidly increased in human myocardial tissue after *ex vivo* exposure to NADPH (100μmol/L, Online Figure V). Incubation of human EpAT and ThAT with MDA had no impact on *ADIPOQ* (Figure 5C), *PPAR-γ* or *CD36* gene expression (Online Figure VII) in either adipose tissue depot. By contrast, exposure of human EpAT to 4HNE induced a rapid 7-fold up-regulation of *ADIPOQ* gene expression, an effect that was prevented by the *PPAR-γ* activity inhibitor T0070907 (Figure 5D). 4HNE also induced a respective 2-fold up-regulation of *PPAR-γ* gene expression (Figure 5E) and a 5-fold increase of its downstream gene, *CD36* (Figure 5F), the latter being prevented by the use of T0070907 (Figure 5F). Interestingly, the expression of *PPAR-γ* was significantly higher in EpAT compared to ThAT, further supporting the notion that its expression in EpAT is largely driven by local signals released from the human myocardium (Online Figure VIII). Taken together, these findings suggest that 4HNE exerts its effects on *ADIPOQ* gene expression not only by up-regulating *PPAR-γ*, but also by enhancing its downstream signalling (Figure 5E-5F). Interestingly, 4HNE had no effect on the expression of *ADIPOQ*, *PPAR-γ* and *CD36* genes in “remote” sites of adipose tissue such as ThAT (Figure 5G-5I), supporting the hypothesis that 4HNE released from the human heart under conditions of increased oxidative stress may activate *PPAR-γ* signalling in EpAT via a paracrine mechanism.

Testing the Paracrine Effects of the Heart on EpAT Using Animal Models

To further explore whether a selective increase in myocardial NADPH-oxidases activity would lead to up-regulation of *ADIPOQ* gene expression in EpAT *in vivo*, we used a transgenic mouse model with cardiomyocyte-specific overexpression of human *NOX2* (*mNOX2-Tg*, Online Figure IX)²⁷ given the strong association of the latter with myocardial redox state in humans (Online Figure X)

Subcutaneous and pericardial AT was collected from twenty-week old male *mNOX2-Tg* and wild-type littermate mice. Overexpression of *NOX2* in the myocardium of these mice (demonstrated in Online Figure IX) resulted in a significant increase of NADPH-oxidases activity, as assessed by both the NADPH-stimulated $O_2^{\cdot -}$ (Figure 6A) and Vas2870-inhibitable $O_2^{\cdot -}$ production (Figure 6B). Overexpression of *NOX2* also led to increased formation of 4HNE -but not MDA- adducts in the myocardium of *mNOX2-Tg* mice (Figure 6C-6D). Interestingly, there was a striking up-regulation of *ADIPOQ* expression in pericardial but not in subcutaneous AT of the *mNOX2-tg* mice (Figure 6E).

Myocardial *NOX2* over-expression also led to increased *ADIPOQ* gene expression in the myocardium (Figure 6F), but did not affect the expression of adiponectin receptors in the myocardium (Figure 6G).

To test whether the findings from the *mNOX2*-Tg mouse model could be replicated in a large animal, with typical EpAT distribution closer to the human one, we used rapid atrial pacing in the pig to increase myocardial $O_2^{\cdot -}$ production. As we have previously shown,⁴ rapid atrial pacing increases myocardial NADPH-oxidase activity in the left atrium as assessed by both the NADPH-stimulated $O_2^{\cdot -}$ and the Vas2870-inhibitable $O_2^{\cdot -}$ signal (Figure 7A-B). Activation of atrial NADPH-oxidase resulted in increased myocardial formation of 4HNE but not MDA adducts (Figure 7C and 7D respectively) and led to a striking up-regulation of *ADIPOQ* expression in EpAT attached to the left atrium, whereas there was no significant effect on *ADIPOQ* expression in the subcutaneous adipose tissue (Figure 7E), nor on the expression of endogenous adiponectin (Figure 7F) or adiponectin receptors (Figure 7G) in the left atrium. Taken together, these data demonstrate that increased NADPH-oxidase activity in the heart leads to up-regulation of *ADIPOQ* expression specifically in EpAT. This corroborates the findings from our cell culture and *ex vivo* work in human atrial tissue and explains the positive associations between *ADIPOQ* expression in EpAT and NADPH-oxidase activity in the underlying myocardium of patients with ischaemic heart disease.

Discussion

In the present study, we explore for the first time in humans, the role of adipose tissue-derived adiponectin in the regulation of myocardial redox state, through modulation of NADPH-oxidase activity. Adiponectin prevents the phosphorylation and membrane translocation of p47^{phox} and prevents Rac1 activation and membrane translocation, both key aspects of myocardial NADPH-oxidase activation. Under conditions of increased myocardial $O_2^{\cdot -}$ generation, oxidation products such as 4HNE can act as signalling molecules from the heart, to activate adiponectin release from EpAT in a PPAR- γ -dependent manner. This introduces the novel concept that, through the release of oxidation products, the human heart regulates key biological processes in adipose tissue by triggering rescue PPAR- γ signalling leading to increased release of adiponectin, which then exerts cardioprotective effects. This novel “inside to outside” signal may be a therapeutic target for the prevention and treatment of redox-dependent cardiac diseases.

Myocardial redox state is a critical determinant of cardiac biology by modulating the function of ion channels, sarcoplasmic reticulum calcium release channels and myofilament proteins, in cardiomyocytes.^{1, 2, 28} $O_2^{\cdot -}$ causes damage to cell membranes and leads to cardiomyocyte necrosis and apoptosis,^{2, 29} while redox-sensitive signalling pathways control fibrotic and hypertrophic responses.³⁰ NADPH-oxidases and particularly Nox2, are major contributors to $O_2^{\cdot -}$ production in the cardiovascular system,³¹ leading to the development of multiple cardiac pathologies such as heart failure,³⁰ myocardial hypertrophy,⁶ atrial fibrillation³⁻⁵ and others. Nox2 activation is dependent on Rac1 binding with Guanosine-5'-triphosphate (GTP) as well as p47^{phox} phosphorylation and their subsequent translocation to the membrane to form the active catalytic complex of the enzyme.³² In this study, we demonstrate that systemic oxidative stress (as characterised by plasma MDA) is not significantly correlated with NADPH-oxidase activity in human myocardium, confirming our previous observation that myocardial redox state is independent of markers of systemic oxidative stress and may be subjected to local, largely unknown regulatory mechanisms.³³

Human adipose tissue secretes a wide range of adipocytokines able to affect myocardial biology.^{16, 34} In addition, EpAT has been proposed to exert paracrine effects on the underlying epicardial coronaries.³⁵ Given the close anatomical relationship between myocardium and EpAT in humans (with adipose tissue penetrating into the heart muscle), it seems that EpAT exerts paracrine effects on the underlying myocardium affecting its biology, as recently demonstrated in some elegant translational studies by Greulich et al.³⁴ Adiponectin appears to have some direct effects on myocardial redox state in animal and cell culture models,^{29, 36} but its role in the regulation of redox state in the human heart is unknown. It is also unclear whether adiponectin produced in EpAT has any paracrine role in the regulation of myocardial redox state, as suggested above.

In this study, we first evaluated the association between myocardial NADPH-oxidases activity and circulating adiponectin or the expression of adiponectin from EpAT or ThAT in a cohort of patients

with ischaemic heart disease. Paradoxically, we observed a positive association between myocardial NADPH-stimulated $O_2^{\cdot-}$ and circulating adiponectin as well as *ADIPOQ* gene expression in EpAT. A similar positive association was also observed between myocardial NADPH-stimulated $O_2^{\cdot-}$ and adiponectin receptor AdipoR1. As this was the first study exploring the role of adiponectin in the regulation of myocardial redox state in humans, we then tried to explore the direction of that unexpected association. By taking advantage of the genetic variability of *ADIPOQ* gene described in recent genome wide association studies^{25,37} we observed that genetically determined reduction of adiponectin levels is also associated with increased NADPH-stimulated $O_2^{\cdot-}$ in the heart of patients with ischaemic heart disease (an association independent of other covariates, including BNP), implying that low adiponectin production in the human AT is causally associated with higher myocardial NADPH-oxidases activity. Using an *ex vivo* model of human myocardium, we observed that adiponectin had a direct inhibitory effect on myocardial NADPH-oxidases activity (evidenced by a reduction in Vas2870-inhibitable myocardial $O_2^{\cdot-}$) and that this effect is mediated by the activation of AMPK leading to reduced phosphorylation and membrane translocation of NADPH-oxidase subunit p47^{phox} in parallel to an AMPK-mediated suppression of Rac1 activation and membrane translocation. This is the first study defining the molecular mechanisms by which adiponectin suppresses NADPH-oxidase activity in the human heart, but these findings are still unable to explain the positive association observed between myocardial redox state and *ADIPOQ* gene expression in EpAT in patients with ischaemic heart disease.

In advanced cardiovascular disease states (i.e. heart failure), circulating adiponectin is significantly elevated.³⁸ In cell culture studies,³⁷ it was demonstrated that adipocytes respond to exogenous BNP (which is significantly elevated in heart failure) by up-regulating *ADIPOQ* gene expression and we have recently demonstrated that this stimulatory effect of BNP on human adipose tissue overrides the suppressive effect of inflammation on the expression and release of adiponectin.¹⁹ Although BNP appears to drive the circulating adiponectin level in the presence of heart failure, its role in the regulation of adipose tissue biology in the absence of heart failure seems less important.¹⁹ In this study, we demonstrate that both circulating adiponectin and *ADIPOQ* gene expression in EpAT are positively correlated with myocardial redox state (and specifically NADPH-oxidase activity), independently of plasma BNP. Importantly, we demonstrate for the first time that products of oxidation, such as 4HNE, which is produced in the human heart under conditions of increased oxidative stress and can cross cellular membranes and act as signalling molecules,³⁹ up-regulates *ADIPOQ* gene expression in the human EpAT via a PPAR- γ dependent mechanism. This novel concept was demonstrated by co-culturing human EpAT with differentiated H9c2 cells after stimulation of cellular $O_2^{\cdot-}$ production by supplying the NADPH-oxidase with its substrate, i.e. NADPH. This finding was then confirmed using a cardiomyocyte-specific *NOX2* transgenic mouse and a pig model of rapid atrial pacing (as means to increase NADPH-oxidases activity and $O_2^{\cdot-}$ generation in the atrial myocardium). Interestingly, in all models it was consistently demonstrated that under conditions of increased myocardial $O_2^{\cdot-}$ generation, the myocardium releases transferable factor(s) (one of which appears to be 4HNE), which then activates PPAR- γ signalling and up-regulates adiponectin expression specifically in the neighbouring EpAT but not in other “remote” adipose tissue depots such as ThAT. Up-regulation of adiponectin in EpAT represents a protective paracrine response of EpAT against myocardial oxidative stress, by inhibiting myocardial NADPH-oxidase. With these findings, we document that EpAT hosts local defence mechanisms protecting the heart against oxidative stress (Online Figure XI).

Our study has some limitations. The patients included into the Clinical Associations and the *ex vivo* study arms were matched for age and gender, but there are some differences in other demographics and risk factor profile. Although we do not perform any direct comparisons between the two study arms, any extrapolations of the results from the *ex vivo* study arm to the Clinical Associations Studies should be made with caution. Moreover, the use of compound C for pharmacological inhibition of AMPK has been criticised due to possible non-AMPK specific effects,⁴⁰ nevertheless it remains the most widely used cell-permeable AMPK-inhibitor in cell/tissue experiments. We hypothesised that the lack of any effects of increased myocardial $O_2^{\cdot-}$ generation/4-HNE release on subcutaneous adipose tissue is due to its “remote” anatomical site, but it could be also related to local depot-specific mechanisms maintaining increased *ADIPOQ* expression in this, preventing any further upregulation of *ADIPOQ* by exogenous 4-HNE.¹⁹ Finally, although we have shown that exogenous NADPH increases intracellular NADPH and stimulates $O_2^{\cdot-}$ generation from NADPH oxidases, these enzymes have their NADPH-binding site intracellularly,⁴¹⁻⁴³ and as NADPH is a large and charged molecule, it is unlikely to cross the plasma

membranes by simple diffusion. Therefore the exact mechanism by which exogenous NADPH triggers O_2^- generation from NADPH-oxidases in H9c2 cells used in the co-culture experiment with rat epicardial fat is unclear. The use of the PMA as a stimulus for O_2^- generation in H9C2 cells (which is known to stimulate NADPH oxidases in a PKC-mediated mechanism) has also direct effects on PPAR- γ signalling in the rat epicardial adipose tissue, therefore the result from that experiment should be interpreted with caution.

In conclusion, we demonstrate for the first time that adiponectin inhibits NADPH-oxidase in the human myocardium via an AMPK/Rac1/p47^{phox}-mediated signaling. We also show that under conditions of increased myocardial oxidative stress, the heart releases transferable mediators (e.g. products of oxidation such as 4HNE), which may diffuse to EpAT leading to PPAR- γ -dependent up-regulation of adiponectin expression in EpAT. This feedback loop represents a novel defence mechanism of the human heart against myocardial oxidative stress, and may prove to be a rational therapeutic target in cardiac disease.

Funding Sources: This work was supported by a Marie Curie Intra European Fellowship by European Commission within the 7th Framework Programme Research (Acronym Project HRS-EAT, #300289) and by grants from the British Heart Foundation Centre of Research Excellence-Oxford (RE/08/004), the British Heart Foundation (FS/11/66/28855, PG/13/56/30383 and RG/11/15/29375), the King's College London British Heart Foundation Centre of Research Excellence (RE/13/2/30182) and by the National Institute for Health Research (NIHR) Oxford Biomedical Research Centre.

Disclosures: None

References

1. Mihm MJ, Yu F, Carnes CA, Reiser PJ, McCarthy PM, Van Wagoner DR and Bauer JA. Impaired myofibrillar energetics and oxidative injury during human atrial fibrillation. *Circulation*. 2001;104:174-80.
2. Lassegue B, San Martin A and Griendling KK. Biochemistry, physiology, and pathophysiology of NADPH oxidases in the cardiovascular system. *Circ Res*. 2012;110:1364-90.
3. Kim YM, Guzik TJ, Zhang YH, Zhang MH, Kattach H, Ratnatunga C, Pillai R, Channon KM and Casadei B. A myocardial Nox2 containing NAD(P)H oxidase contributes to oxidative stress in human atrial fibrillation. *Circ Res*. 2005;97:629-36.
4. Reilly SN, Jayaram R, Nahar K, Antoniadou C, Verheule S, Channon KM, Alp NJ, Schotten U and Casadei B. Atrial sources of reactive oxygen species vary with the duration and substrate of atrial fibrillation: implications for the antiarrhythmic effect of statins. *Circulation*. 2011;124:1107-17.
5. Antoniadou C, Demosthenous M, Reilly S, Margaritis M, Zhang MH, Antonopoulos A, Marinou K, Nahar K, Jayaram R, Tousoulis D, Bakogiannis C, Sayeed R, Triantafyllou C, Koumallos N, Psarros C, Miliou A, Stefanadis C, Channon KM and Casadei B. Myocardial redox state predicts in-hospital clinical outcome after cardiac surgery effects of short-term pre-operative statin treatment. *J Am Coll Cardiol*. 2012;59:60-70.
6. Murdoch CE, Zhang M, Cave AC and Shah AM. NADPH oxidase-dependent redox signalling in cardiac hypertrophy, remodelling and failure. *Cardiovasc Res*. 2006;71:208-15.
7. Sorescu D and Griendling KK. Reactive oxygen species, mitochondria, and NAD(P)H oxidases in the development and progression of heart failure. *Congest Heart Fail*. 2002;8:132-40.
8. Montezano AC and Touyz RM. Reactive oxygen species, vascular Noxs, and hypertension: focus on translational and clinical research. *Antioxid Redox Signal*. 2014;20:164-82.
9. Cosentino F, Eto M, De Paolis P, van der Loo B, Bachschmid M, Ullrich V, Kouroedov A, Delli Gatti C, Joch H, Volpe M and Luscher TF. High glucose causes upregulation of cyclooxygenase-2 and alters prostanoid profile in human endothelial cells: role of protein kinase C and reactive oxygen species. *Circulation*. 2003;107:1017-23.
10. Paneni F, Beckman JA, Creager MA and Cosentino F. Diabetes and vascular disease: pathophysiology, clinical consequences, and medical therapy: part I. *Eur Heart J*. 2013;34:2436-43.
11. Paneni F, Costantino S and Cosentino F. Insulin resistance, diabetes, and cardiovascular risk. *Curr Atheroscler Rep*. 2014;16:419.
12. Kjekshus J, Apetrei E, Barrios V, Bohm M, Cleland JG, Cornel JH, Dunselman P, Fonseca C, Goudev A, Grande P, Gullestad L, Hjalmarson A, Hradec J, Janosi A, Kamensky G, Komajda M, Korewicki J, Kuusi T, Mach F, Mareev V, McMurray JJ, Ranjith N, Schaufelberger M, Vanhaecke J, van Veldhuisen DJ, Waagstein F, Wedel H and Wikstrand J. Rosuvastatin in older patients with systolic heart failure. *N Engl J Med*. 2007;357:2248-61.
13. San Martin A and Griendling KK. NADPH oxidases: progress and opportunities. *Antioxid Redox Signal*. 2014;20:2692-4.
14. Antonopoulos AS, Margaritis M, Coutinho P, Digby J, Patel R, Psarros C, Ntusi N, Karamitsos TD, Lee R, De Silva R, Petrou M, Sayeed R, Demosthenous M, Bakogiannis C, Wordsworth PB, Tousoulis D, Neubauer S, Channon KM and Antoniadou C. Reciprocal Effects of Systemic Inflammation and Brain Natriuretic Peptide on Adiponectin Biosynthesis in Adipose Tissue of Patients With Ischemic Heart Disease. *Arterioscler Thromb Vasc Biol*. 2014.
15. Touyz RM. Endothelial cell IL-8, a new target for adiponectin: implications in vascular protection. *Circ Res*. 2005;97:1216-9.
16. Antoniadou C, Antonopoulos AS, Tousoulis D and Stefanadis C. Adiponectin: from obesity to cardiovascular disease. *Obes Rev*. 2009;10:269-79.
17. Shibata R, Sato K, Pimentel DR, Takemura Y, Kihara S, Ohashi K, Funahashi T, Ouchi N and Walsh K. Adiponectin protects against myocardial ischemia-reperfusion injury through AMPK- and COX-2-dependent mechanisms. *Nat Med*. 2005;11:1096-103.

18. Koenig W, Khuseynova N, Baumert J, Meisinger C and Lowel H. Serum concentrations of adiponectin and risk of type 2 diabetes mellitus and coronary heart disease in apparently healthy middle-aged men: results from the 18-year follow-up of a large cohort from southern Germany. *J Am Coll Cardiol.* 2006;48:1369-77.
19. Antonopoulos AS, Margaritis M, Coutinho P, Digby J, Patel R, Psarros C, Ntusi N, Karamitsos TD, Lee R, De Silva R, Petrou M, Sayeed R, Demosthenous M, Bakogiannis C, Wordsworth PB, Tousoulis D, Neubauer S, Channon KM and Antoniades C. Reciprocal effects of systemic inflammation and brain natriuretic peptide on adiponectin biosynthesis in adipose tissue of patients with ischemic heart disease. *Arterioscler Thromb Vasc Biol.* 2014;34:2151-9.
20. Schnabel R, Messow CM, Lubos E, Espinola-Klein C, Rupprecht HJ, Bickel C, Sinning C, Tzikas S, Keller T, Genth-Zotz S, Lackner KJ, Munzel TF and Blankenberg S. Association of adiponectin with adverse outcome in coronary artery disease patients: results from the AtheroGene study. *Eur Heart J.* 2008;29:649-57.
21. Margaritis M, Antonopoulos AS, Digby J, Lee R, Reilly S, Coutinho P, Shirodaria C, Sayeed R, Petrou M, De Silva R, Jalilzadeh S, Demosthenous M, Bakogiannis C, Tousoulis D, Stefanadis C, Choudhury RP, Casadei B, Channon KM and Antoniades C. Interactions between vascular wall and perivascular adipose tissue reveal novel roles for adiponectin in the regulation of endothelial nitric oxide synthase function in human vessels. *Circulation.* 2013;127:2209-21.
22. Wingler K, Altenhoefer SA, Kleikers PW, Radermacher KA, Kleinschnitz C and Schmidt HH. VAS2870 is a pan-NADPH oxidase inhibitor. *Cell Mol Life Sci.* 2012;69:3159-60.
23. Antoniades C, Bakogiannis C, Tousoulis D, Reilly S, Zhang MH, Paschalis A, Antonopoulos AS, Demosthenous M, Miliou A, Psarros C, Marinou K, Sfyas N, Economopoulos G, Casadei B, Channon KM and Stefanadis C. Preoperative atorvastatin treatment in CABG patients rapidly improves vein graft redox state by inhibition of Rac1 and NADPH-oxidase activity. *Circulation.* 2010;122:S66-73.
24. Brewer AC, Murray TV, Arno M, Zhang M, Anilkumar NP, Mann GE and Shah AM. Nox4 regulates Nrf2 and glutathione redox in cardiomyocytes in vivo. *Free Radic Biol Med.* 2011;51:205-15.
25. Heid IM, Henneman P, Hicks A, Coassin S, Winkler T, Aulchenko YS, Fuchsberger C, Song K, Hivert MF, Waterworth DM, Timpson NJ, Richards JB, Perry JR, Tanaka T, Amin N, Kollerits B, Pichler I, Oostra BA, Thorand B, Frants RR, Illig T, Dupuis J, Glaser B, Spector T, Guralnik J, Egan JM, Florez JC, Evans DM, Soranzo N, Bandinelli S, Carlson OD, Frayling TM, Burling K, Smith GD, Mooser V, Ferrucci L, Meigs JB, Vollenweider P, Dijk KW, Pramstaller P, Kronenberg F and van Duijn CM. Clear detection of ADIPOQ locus as the major gene for plasma adiponectin: results of genome-wide association analyses including 4659 European individuals. *Atherosclerosis.* 2010;208:412-20.
26. Richards JB, Waterworth D, O'Rahilly S, Hivert MF, Loos RJ, Perry JR, Tanaka T, Timpson NJ, Semple RK, Soranzo N, Song K, Rocha N, Grundberg E, Dupuis J, Florez JC, Langenberg C, Prokopenko I, Saxena R, Sladek R, Aulchenko Y, Evans D, Waeber G, Erdmann J, Burnett MS, Sattar N, Devaney J, Willenborg C, Hingorani A, Witteman JC, Vollenweider P, Glaser B, Hengstenberg C, Ferrucci L, Melzer D, Stark K, Deanfield J, Winogradow J, Grassl M, Hall AS, Egan JM, Thompson JR, Ricketts SL, Konig IR, Reinhard W, Grundy S, Wichmann HE, Barter P, Mahley R, Kesaniemi YA, Rader DJ, Reilly MP, Epstein SE, Stewart AF, Van Duijn CM, Schunkert H, Burling K, Deloukas P, Pastinen T, Samani NJ, McPherson R, Davey Smith G, Frayling TM, Wareham NJ, Meigs JB, Mooser V, Spector TD and Consortium G. A genome-wide association study reveals variants in ARL15 that influence adiponectin levels. *PLoS Genet.* 2009;5:e1000768.
27. Zhang M, Prosser BL, Bamboye MA, Gondim AN, Santos CX, Martin D, Ghigo A, Perino A, Brewer AC, Ward CW, Hirsch E, Lederer WJ and Shah AM. Contractile Function During Angiotensin-II Activation: Increased Nox2 Activity Modulates Cardiac Calcium Handling via Phospholamban Phosphorylation. *J Am Coll Cardiol.* 2015;66:261-72.
28. Kohr MJ, Traynham CJ, Roof SR, Davis JP and Ziolo MT. cAMP-independent activation of protein kinase A by the peroxynitrite generator SIN-1 elicits positive inotropic effects in cardiomyocytes. *J Mol Cell Cardiol.* 2010;48:645-8.

29. Park M, Youn B, Zheng XL, Wu D, Xu A and Sweeney G. Globular adiponectin, acting via AdipoR1/APPL1, protects H9c2 cells from hypoxia/reoxygenation-induced apoptosis. *PLoS One*. 2011;6:e19143.
30. Parajuli N, Patel VB, Wang W, Basu R and Oudit GY. Loss of NOX2 (gp91phox) prevents oxidative stress and progression to advanced heart failure. *Clin Sci (Lond)*. 2014;127:331-40.
31. Brown DI and Griendling KK. Nox proteins in signal transduction. *Free Radic Biol Med*. 2009;47:1239-53.
32. Mizrahi A, Berdichevsky Y, Casey PJ and Pick E. A prenylated p47phox-p67phox-Rac1 chimera is a Quintessential NADPH oxidase activator: membrane association and functional capacity. *J Biol Chem*. 2010;285:25485-99.
33. Kim YM, Kattach H, Ratnatunga C, Pillai R, Channon KM and Casadei B. Association of atrial nicotinamide adenine dinucleotide phosphate oxidase activity with the development of atrial fibrillation after cardiac surgery. *J Am Coll Cardiol*. 2008;51:68-74.
34. Greulich S, Maxhera B, Vandenplas G, de Wiza DH, Smiris K, Mueller H, Heinrichs J, Blumensatt M, Cuvelier C, Akhyari P, Ruige JB, Ouwens DM and Eckel J. Secretory products from epicardial adipose tissue of patients with type 2 diabetes mellitus induce cardiomyocyte dysfunction. *Circulation*. 2012;126:2324-34.
35. Konishi M, Sugiyama S, Sato Y, Oshima S, Sugamura K, Nozaki T, Ohba K, Matsubara J, Sumida H, Nagayoshi Y, Sakamoto K, Utsunomiya D, Awai K, Jinnouchi H, Matsuzawa Y, Yamashita Y, Asada Y, Kimura K, Umemura S and Ogawa H. Pericardial fat inflammation correlates with coronary artery disease. *Atherosclerosis*. 2010;213:649-55.
36. Wang Y, Tao L, Yuan Y, Lau WB, Li R, Lopez BL, Christopher TA, Tian R and Ma XL. Cardioprotective effect of adiponectin is partially mediated by its AMPK-independent antinitrative action. *Am J Physiol Endocrinol Metab*. 2009;297:E384-91.
37. Tsukamoto O, Fujita M, Kato M, Yamazaki S, Asano Y, Ogai A, Okazaki H, Asai M, Nagamachi Y, Maeda N, Shintani Y, Minamino T, Asakura M, Kishimoto I, Funahashi T, Tomoike H and Kitakaze M. Natriuretic peptides enhance the production of adiponectin in human adipocytes and in patients with chronic heart failure. *J Am Coll Cardiol*. 2009;53:2070-7.
38. George J, Patal S, Wexler D, Sharabi Y, Peleg E, Kamari Y, Grossman E, Sheps D, Keren G and Roth A. Circulating adiponectin concentrations in patients with congestive heart failure. *Heart*. 2006;92:1420-4.
39. Ayala A, Munoz MF and Arguelles S. Lipid peroxidation: production, metabolism, and signaling mechanisms of malondialdehyde and 4-hydroxy-2-nonenal. *Oxid Med Cell Longev*. 2014;2014:360438.
40. Viollet B, Horman S, Leclerc J, Lantier L, Foretz M, Billaud M, Giri S and Andreelli F. AMPK inhibition in health and disease. *Crit Rev Biochem Mol Biol*. 2010;45:276-95.
41. Park L, Anrather J, Zhou P, Frys K, Wang G and Iadecola C. Exogenous NADPH increases cerebral blood flow through NADPH oxidase-dependent and -independent mechanisms. *Arterioscler Thromb Vasc Biol*. 2004;24:1860-5.
42. Didion SP and Faraci FM. Effects of NADH and NADPH on superoxide levels and cerebral vascular tone. *Am J Physiol Heart Circ Physiol*. 2002;282:H688-95.
43. Guzik TJ, West NE, Black E, McDonald D, Ratnatunga C, Pillai R and Channon KM. Vascular superoxide production by NAD(P)H oxidase: association with endothelial dysfunction and clinical risk factors. *Circ Res*. 2000;86:E85-90.

Legends to the Figures

Figure 1. In the Clinical Association arm of the study, high circulating adiponectin levels were paradoxically related with high myocardial NADPH-stimulated superoxide ($O_2^{\cdot-}$) (Panel A) and high plasma malonyldialdehyde (MDA, a marker of systemic oxidative stress, Panel B). There was no association of circulating adiponectin with plasma interleukin 6 (IL-6, Panel C) or C-reactive protein (hsCRP, Panel D). High circulating adiponectin was also positively related with high plasma B-natriuretic peptide (BNP, Panel E). Values are expressed as median [25th-75th percentile].

Figure 2. The total number of rs17366568G alleles (polymorphism in *ADIPOQ* gene) and rs266717T alleles (polymorphism in *ADIPOQ* gene promoter) had an additive effect on circulating adiponectin levels (Panel A) and was associated with reduced NADPH-stimulated superoxide ($O_2^{\cdot-}$) in human myocardium (Panel B). The number of rs17366568G/rs266717T alleles was positively associated with higher *ADIPOQ* gene expression in thoracic adipose tissue (ThAT, Panel C), but not associated in epicardial adipose tissue (EpAT, Panel D). Patients with higher *ADIPOQ* (Panel E) or PPAR- γ (Panel F) gene expression in EpAT also had higher NADPH-stimulated $O_2^{\cdot-}$ production in their myocardium. Higher myocardial NADPH-stimulated $O_2^{\cdot-}$ was not associated with endogenous *ADIPOQ* gene expression in the heart (Panel G), but was associated with higher gene expression of adiponectin receptor-1 (AdipoR1), but not of AdipoR2 or T-cadherin (CDH13) in human myocardial tissue (Panel H). Values are expressed as median [25th-75th percentile].

Figure 3. *Ex vivo* incubation of human myocardium with adiponectin (AdN, 10ug/ml) for 2 hours resulted in increased phosphorylation of AMPK α at Thr172 (p-AMPK, Panel A) leading to AMPK activation as assessed by the phosphorylation status of its downstream target acetyl-CoA carboxylase (ACC) at Ser79 (p-ACC, Panel B), an effect reversed by Compound-C (10uM, Panel A & B). Adiponectin reduced superoxide ($O_2^{\cdot-}$) production in human myocardium (Panel C) and specifically NADPH oxidase activity, as assessed by measuring the Vas2870-inhibitable (40 μ mol/L) $O_2^{\cdot-}$ (Panel D); both effects were reversed by Compound-C (Panels C & D). These effects of adiponectin on myocardial $O_2^{\cdot-}$ were also confirmed by dihydroethidium (DHE) staining; adiponectin reduced both total and Vas2870-inhibitable DHE fluorescence and these effects were reversed by Compound-C (Panels E to G). Importantly, adiponectin prevented Rac1 activation (assessed by measuring the ratio of Guanosine-5'-triphosphate (GTP)-Rac1 to total Rac1 (t-Rac1, Panel H) and reduced the membrane-bound fraction of Rac1 (m-Rac1, Panel I); both effects were reversed by Compound-C. Similarly, adiponectin prevented p47^{phox} phosphorylation at its activatory site Ser359 (p-p47^{phox}, Panel J) and reduced the membrane-bound fraction of NADPH oxidase subunit p47^{phox} (m-p47^{phox}, Panel K) in an AMPK-dependent manner (as both effects were reversed by Compound-C, Panel J & K). For Panels A and B: adiponectin n=7-13 per group; CC: 4-7 per group; Panels C, D, H, J, K: adiponectin group: n=7-12, CC group: n=4-6; Panel E, F, G, I: n=3-4 per group. Values are expressed as fold change vs control group and shown as mean \pm SEM; *p<0.05, **p<0.01 vs control.

Figure 4. To examine whether under conditions of increased endogenous oxidative stress cardiomyocytes release a transferable factor able to affect the activation of PPAR- γ /adiponectin signalling in rat epicardial adipose tissue (EpAT), we exposed H9c2 cells (differentiated to cardiomyocytes) to NADPH 100 μ mol/L for 2 hours while rat EpAT was conditioned *ex vivo* (Panel A). After 2h, the rat EpAT was transferred into the H9c2 wells and co-cultured for an additional 16 hours (Panel A). At the end of the incubation period, gene expression was studied in the rat EpAT. Addition of NADPH to intact H9c2 cells grown on coverslips led to a striking increase of NADPH oxidases-derived superoxide ($O_2^{\cdot-}$) that was partly inhibitable by either Vas2870 (a pan-Nox inhibitor) or gp91-dstat (a specific inhibitor of NOX2) (Panel B), as demonstrated by real-time monitoring using lucigenin-enhanced chemiluminescence. Co-incubation of rat EpAT with H9c2 cardiomyocytes stimulated with NADPH resulted in an up-regulation of *ADIPOQ* (Panel C), *PPAR- γ* (Panel D) and *CD36* (Panel E) in EpAT at 16h. All these effects were prevented by PEG-SOD (300 U/ml) or vas2870 (10 nmol/L). The presence of unstimulated H9C2 cells or NADPH alone had no effect on the expression of *ADIPOQ*, *PPAR- γ* or *CD36* genes in the rat EpAT (Panels C-E). DMEM: Dulbecco's Modified Eagle Medium; SOD: Superoxide dismutase; Concentration of gp91-dstat was 50 μ mol/L. Values are presented as

mean \pm SEM. For Panel B: n=7 and for Panels C to E: n=7; *p<0.05 vs control group; ***p<0.0001 vs resting; †P<0.05 vs NADPH alone.

Figure 5. In human myocardium, increased NADPH oxidases activity (upper tertile of NADPH-stimulated O_2^- in the Clinical Associations Studies) were associated with significantly greater 4-hydroxynonenal (4HNE, Panel A) and malonyldialdehyde (MDA, Panel B) production. Incubation of epicardial (EpAT) and thoracic (ThAT) adipose tissue with MDA (1mmol/L) for 16h had no significant impact on *ADIPOQ* gene expression (Panel C). On the contrary, incubation of EpAT with 4HNE (30 μ mol/L) for 16h induced a striking increase in *ADIPOQ* (Panel D), *PPAR- γ* (Panel E) and *CD36* (Panel F). The effects of 4HNE on *ADIPOQ* and *CD36* gene expression were reversed by the inhibitor of *PPAR- γ* activity, T0070907 (10 μ mol/L Panels D and F). Importantly, 4HNE had no significant impact on the expression of *ADIPOQ* (Panel G), *PPAR- γ* (Panel H) or *CD36* (Panel I) genes in ThAT. Values are represented as fold change compared to control group (means \pm SEM). For Panels A and B: n=4 per group, for Panel C: n=5 per group, for Panels D to I: n=5-8 per group, *p<0.05; **P<0.01 vs low myocardial NADPH-oxidase activity (Panels A and B) or control (Panels C to I).

Figure 6. In the cardiomyocyte-specific *NOX2*-transgenic mouse, myocardial NADPH oxidases were activated, as assessed by both the NADPH-stimulated (Panel A) and Vas2870-inhibitable superoxide (O_2^-) signal (Panels B), and by increased formation of 4-hydroxynonenal (4HNE) protein adducts compared to wild type (wt) animals (Panel C). There was no difference in the myocardial protein levels of malonyldialdehyde (MDA) adducts (Panel D). Increased myocardial oxidative stress and 4HNE adducts formation in *mNOX2*-tg mice led to increased *ADIPOQ* gene expression in the fat attached to the heart (pericardial adipose tissue, PerAT), but not in ‘remote’ AT depots, e.g. subcutaneous AT (ScAT, Panel E). *mNOX2*-tg mice also had increased endogenous levels of *ADIPOQ* gene expression in myocardial tissue (Panel F), but there was no difference in the myocardial gene expression levels of any of adiponectin receptors, T-cadherin (CDH13), AdipoR1 and AdipoR2 (Panel G); for Panels A to E: n=5-6 per group, for Panels F to G: n=9-10 per group, *p<0.05, **p<0.01 vs wild type group.

Figure 7. In a pig model of rapid atrial pacing (RAP), myocardial NADPH oxidases activity was significantly higher in the paced animals as compared to sham, as shown by both the NADPH-stimulated and Vas2870-inhibitable superoxide (O_2^-) signal (Panels A-B). RAP also increased formation of 4HNE (but no MDA) protein adducts (Panels C-D) and upregulated *ADIPOQ* gene expression in epicardial AT (EpAT) but not in “remote” AT depots, e.g. ScAT (Panel E). There was no difference in endogenous *ADIPOQ* gene expression levels in the heart (Panel F) or myocardial expression of adiponectin receptors (Panel G) between sham-operated and RAP animals; for all panels: n=5 per group, *p<0.05, **p<0.01 vs sham group.

Table 1: Demographic characteristics of study participants

	Clinical Associations Studies	<i>Ex Vivo</i> studies
Participants (n)	247	59
Age (years)	66.8±0.6	69.1±1.5
Gender (Males)	200	42
Hypertension (%)	66.9	74.6
Hyperlipidaemia (%)	49.8	79.7*
Diabetes mellitus (%)	32.5	30.5
Smoking (active/ex)	28.2/43.3	13.6/54.2
BMI (kg/m ²)	27.5±0.27	29.5±0.6*
Cholesterol (mmol/L)	4.34±0.2	5.70±0.6*
HDL (mmol/L)	0.94±0.04	1.30±0.20*
Triglycerides (mmol/L)#	1.39 [1.06-1.80]	1.20 [0.80-1.74]
Body surface area (m ²)	1.89±0.18	1.87±0.08
Waist circumference (cm)	99.24±0.85	100.11±1.99
Waist:Hip ratio	1.08±0.02	0.99±0.01*
Glucose (mmol/L)	7.28±0.39	6.39±0.26*
HOMA-IR	5.43±1.65	9.27±1.43*
BNP (pg/ml)	145±29	140±34
Medication		
ACEi/ARBs	49.1/15.0	36.4/7.3
Beta blockers	68.4	63.6
Aspirin/clopidogrel	64.4/44.2	72.7/25.5
Statins	66.2	76.4
CCBs	20.5	32.7*
Diuretics	20.7	25.5

BMI: Body mass index; HDL: High density lipoprotein; HOMA-IR: Homeostatic model of insulin resistance; BNP: Brain natriuretic peptide; ACEi: Angiotensin converting enzyme inhibitors; ARBs: Angiotensin receptor blockers; CCBs: Calcium channel blockers. #values expressed as median [25th-75th percentile]. *p<0.05 vs population in Clinical Associations studies

Novelty and Significance

What is known?

- NADPH oxidases are major contributors to myocardial oxidative stress in humans.
- Epicardial adipose tissue is an endocrine tissue secreting active adipokines
- Adipose tissue-derived adiponectin has beneficial effects on cardiovascular system in experimental animal models

What new information does this article contribute?

- This work demonstrates for the first time that adiponectin suppresses oxidative stress in the human heart
- A novel “inside-to-outside” signal from the heart to its epicardial adipose tissue is described, introducing the concept of a cross-talk between the human heart and its epicardial adipose tissue
- Increased myocardial oxidative stress induces changes in the biology of the adjacent epicardial adipose tissue in humans, triggering local adiponectin expression in epicardial fat
- Modulations in adiponectin produced by epicardial adipose tissue can be considered as a local defense mechanism to protect the heart from oxidative injury.

Summary paragraph. The role of epicardial adipose tissue in the physiology of the human heart is unclear. By using *ex vivo* models of human myocardium from patients with ischaemic heart disease as well as cell culture and animal models, we demonstrate that epicardial adipose tissue responds to the release of oxidation products from the heart by activating peroxisome proliferator-activated receptor- γ (PPAR- γ) signaling, leading to increased local adiponectin biosynthesis (inside-to-outside signal). Local adiponectin released from epicardial adipose tissue may then exert paracrine effects on the human myocardium (outside-to-inside signal), suppressing free radicals production by inhibiting NADPH oxidases. Our data introduce the novel concept that human epicardial adipose tissue is in close, bi-directional communication with the heart and it may host defence mechanisms that protect the myocardium from oxidative assaults. These findings imply that targeting of epicardial adipose tissue may be a rational therapeutic strategy for cardioprotection in ischaemic heart disease.

Figure 1

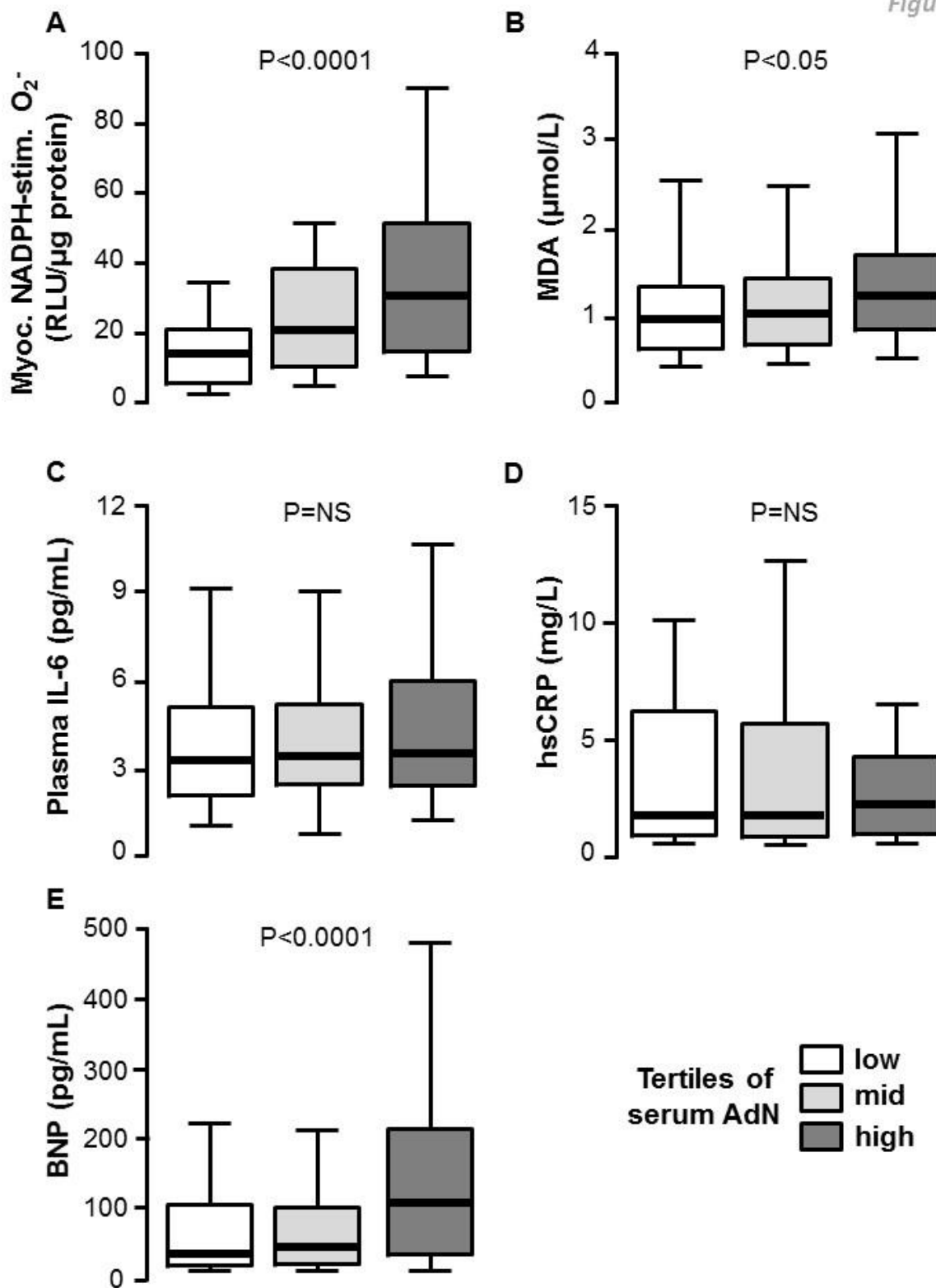
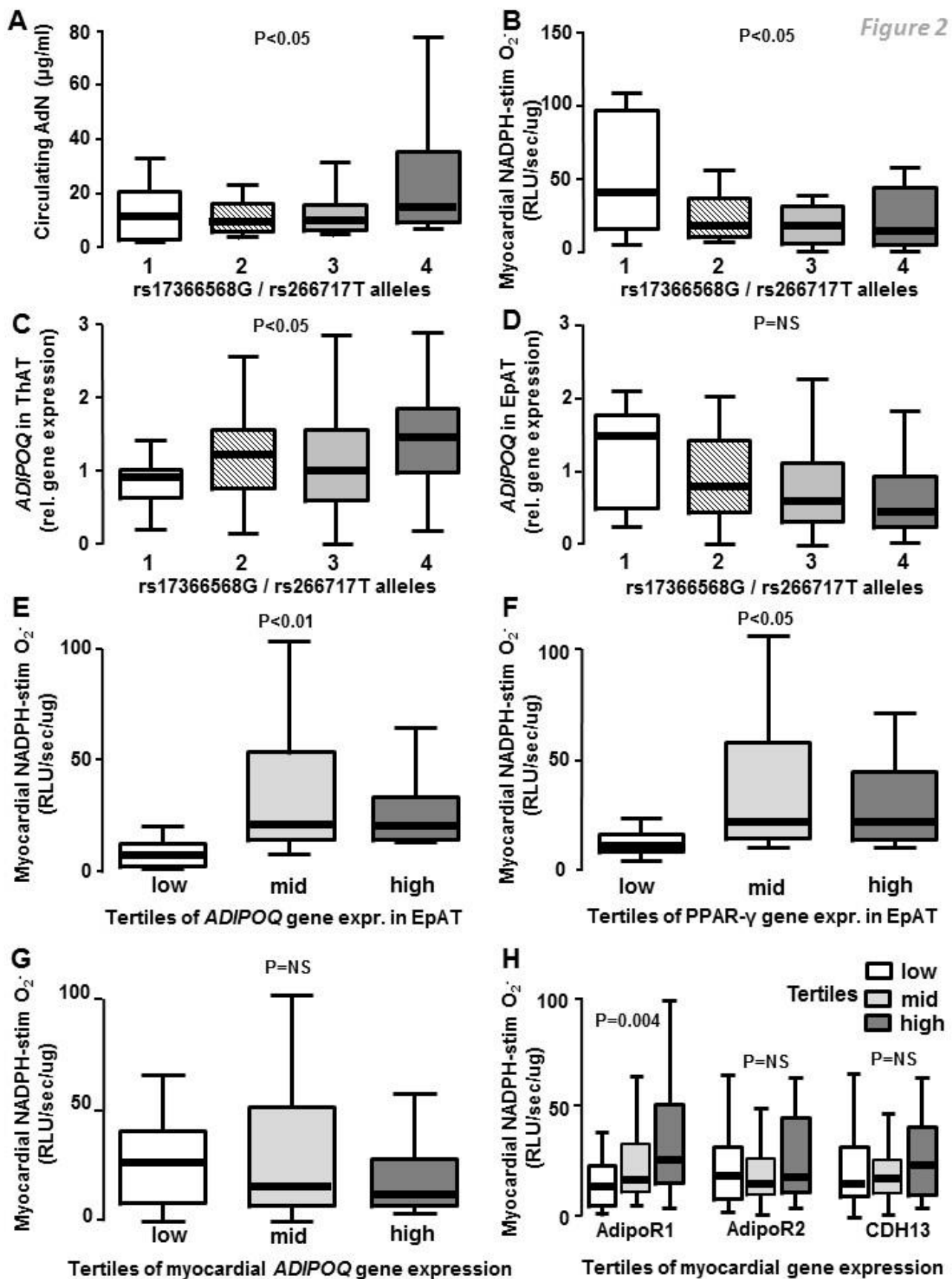


Figure 2



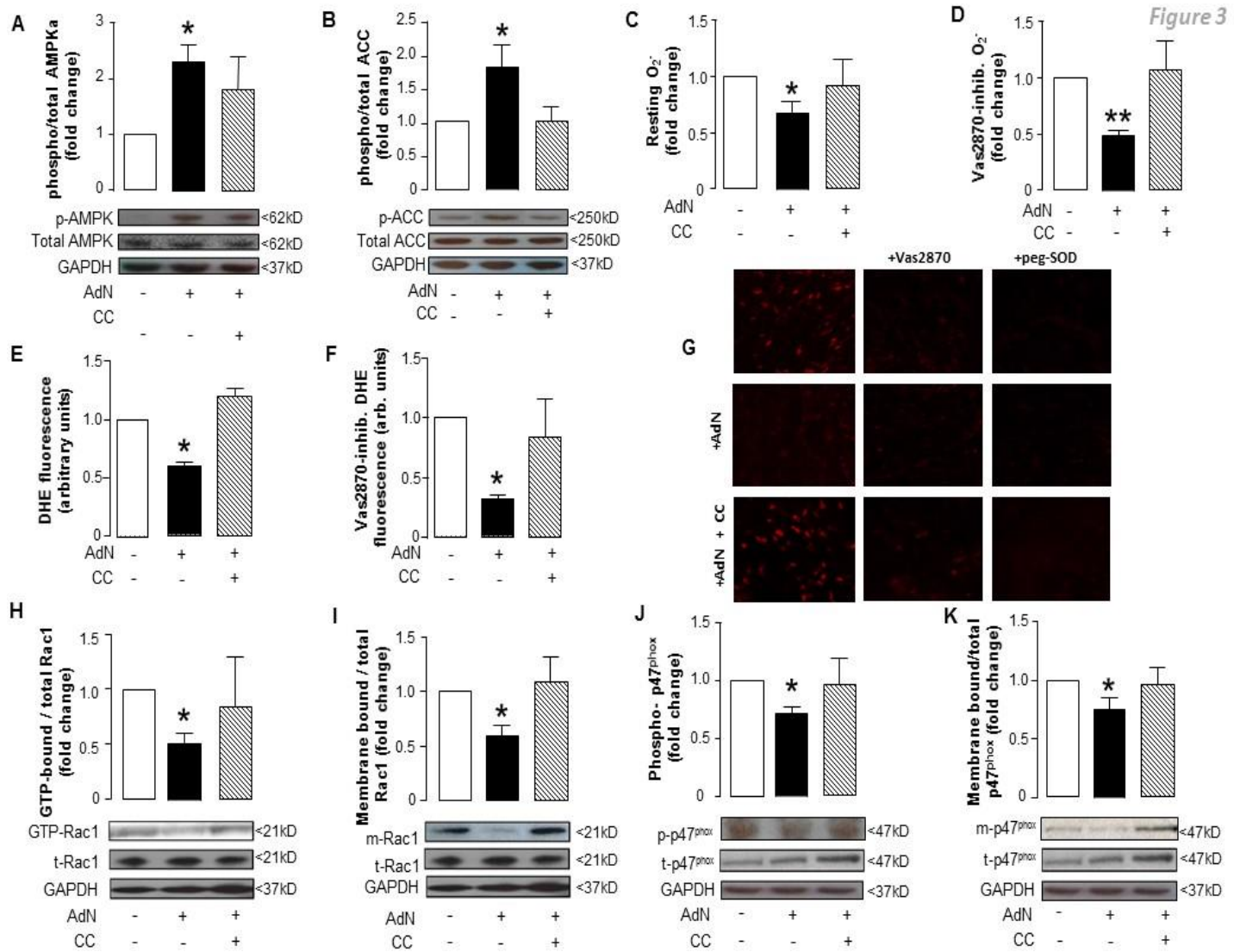


Figure 4

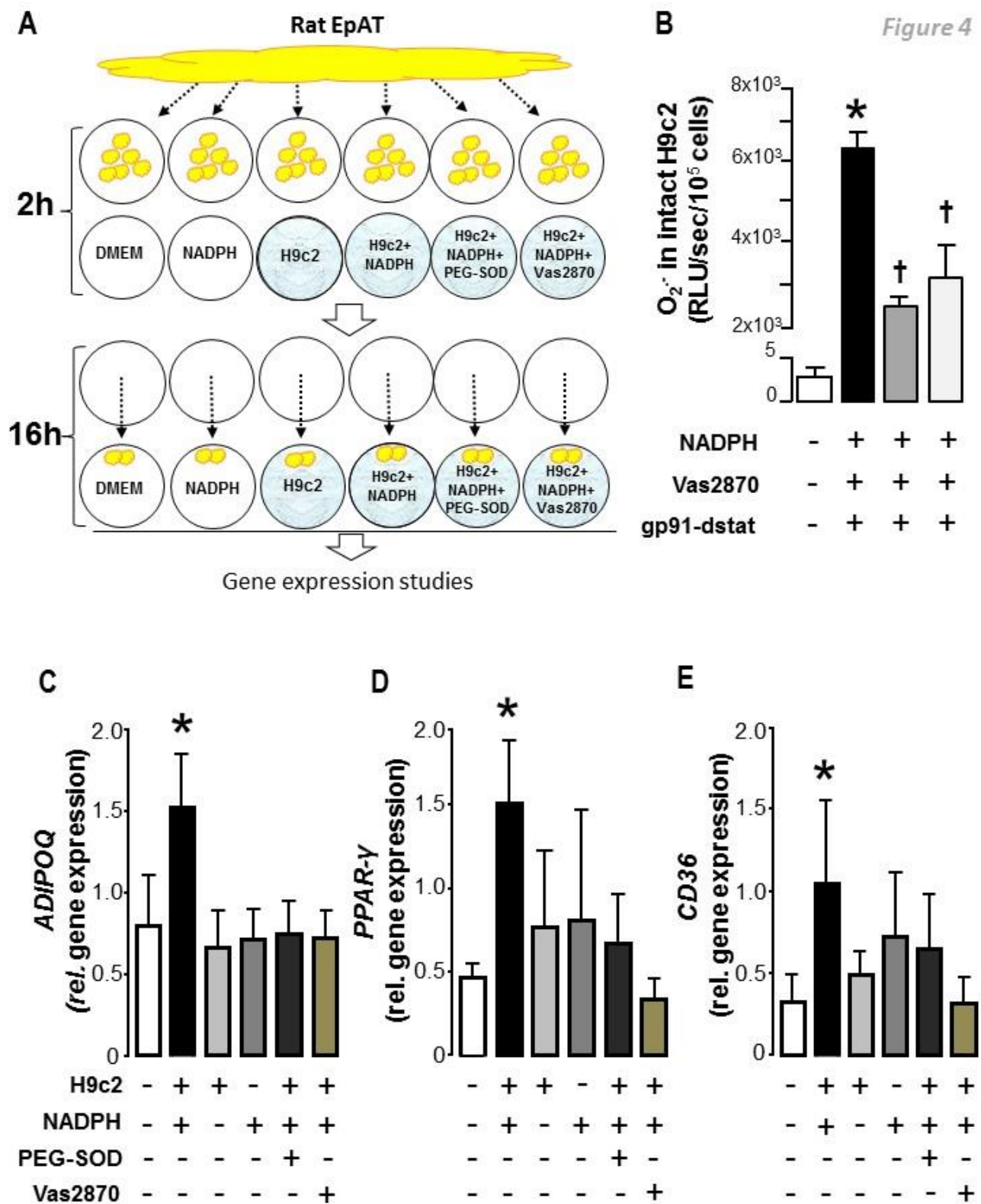
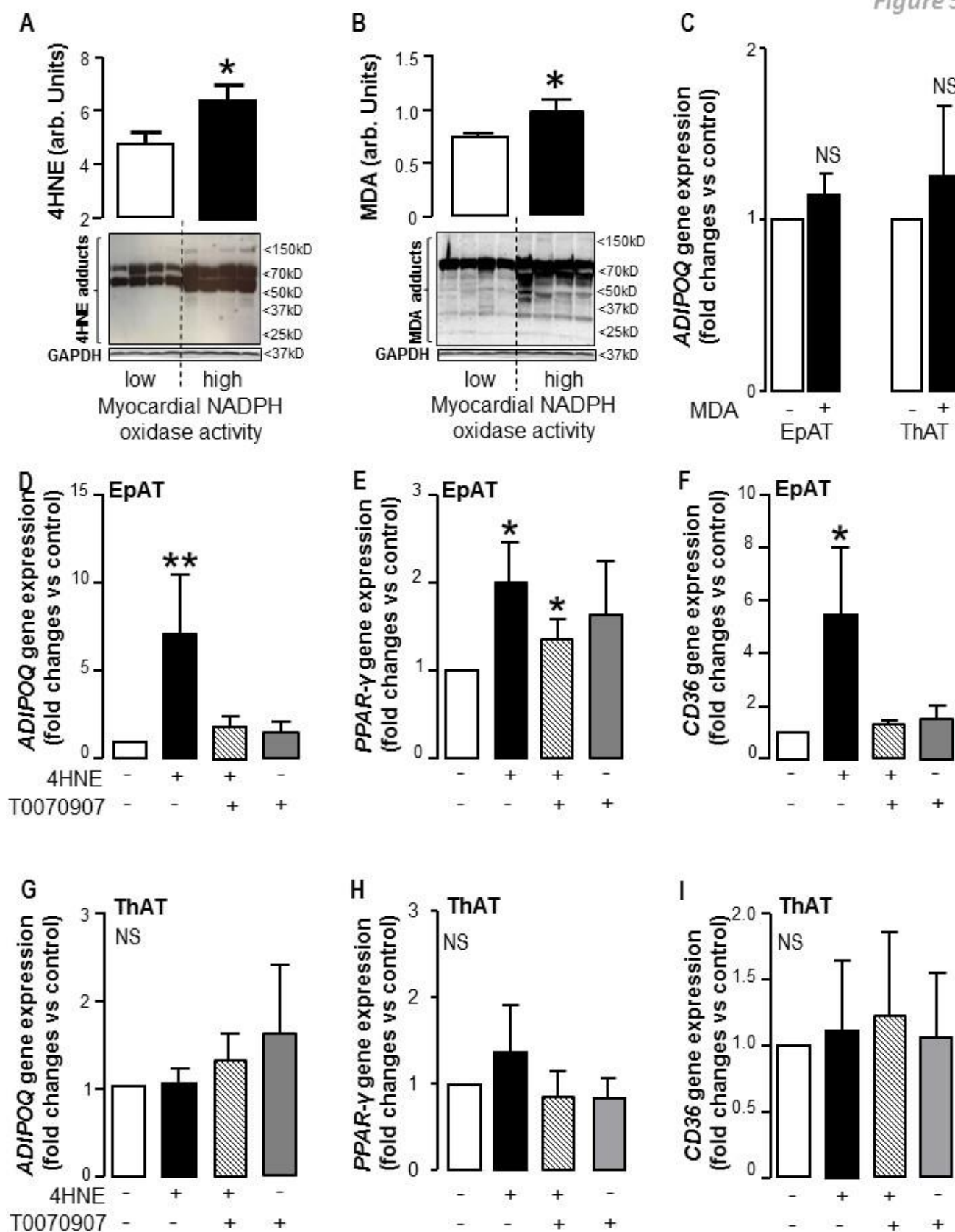
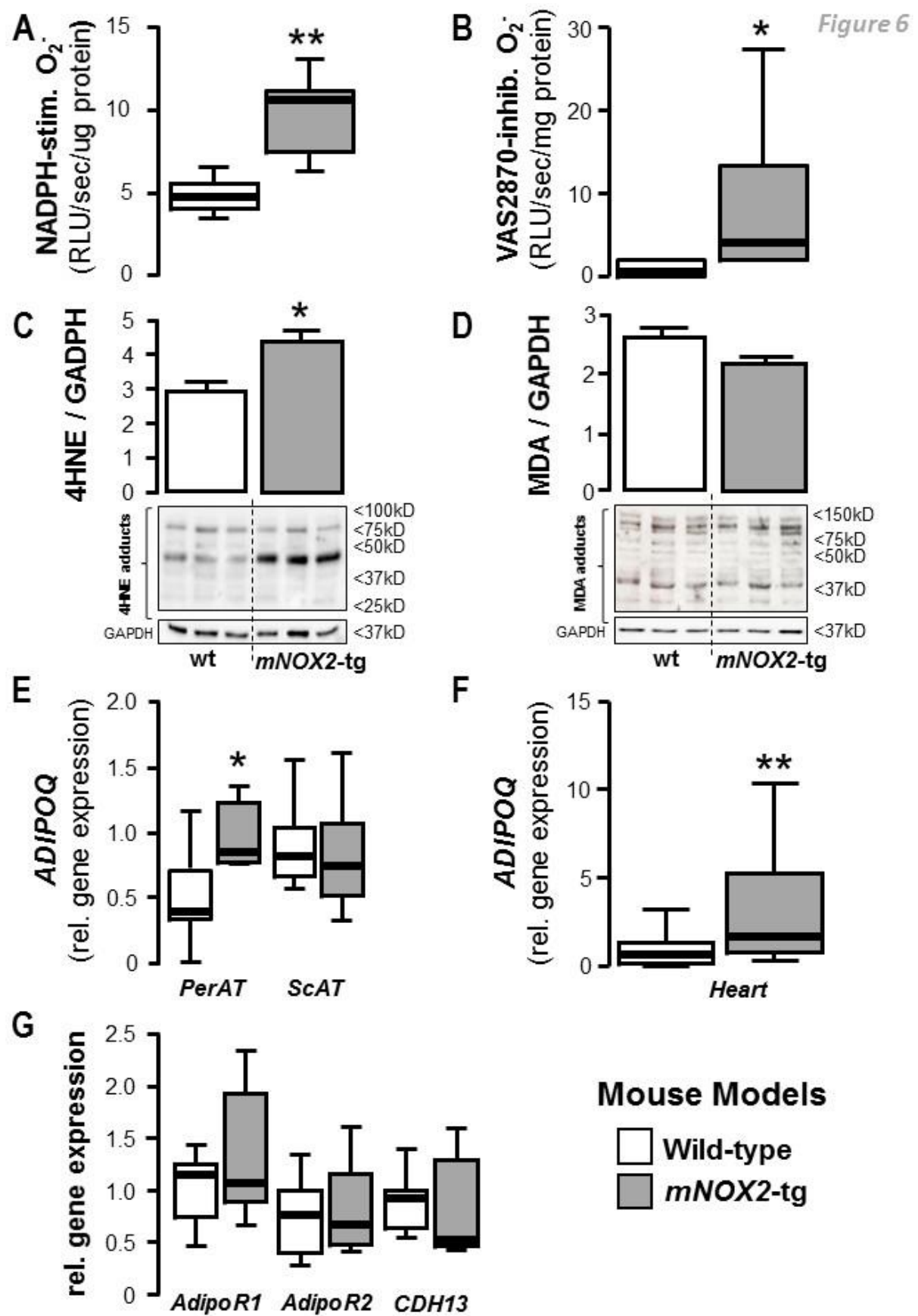
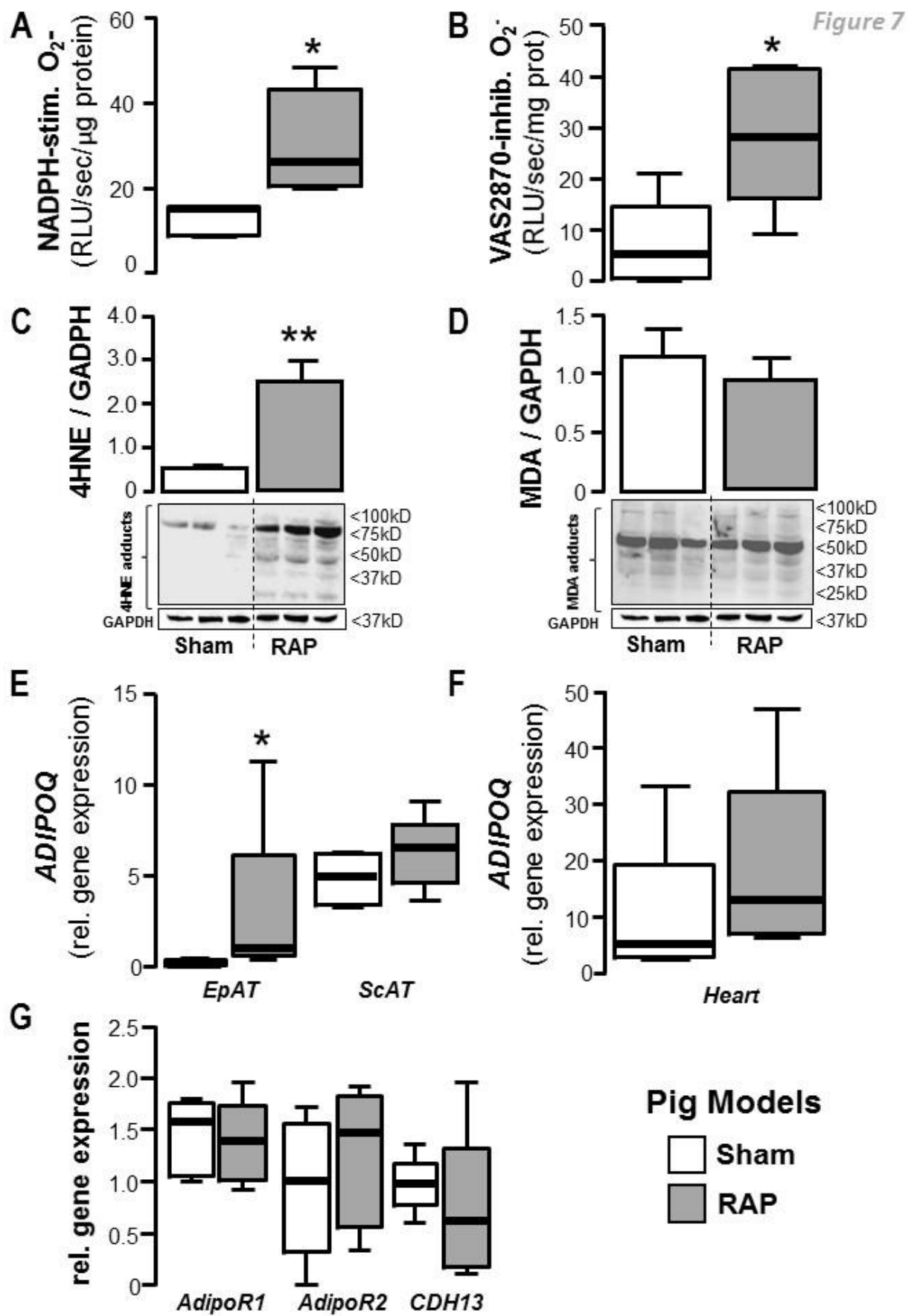


Figure 5







SUPPLEMENTAL MATERIAL**Mutual Regulation of Epicardial Adipose Tissue and Myocardial Redox State
by PPAR- γ /Adiponectin Signalling**

Alexios S. Antonopoulos^a, Marios Margaritis^a, Sander Verheule^b, Alice Recalde^a, Fabio Sanna^a, Laura Herdman^a, Costas Psarros^a, Hussein Nasrallah^b, Patricia Coutinho^a, Ioannis Akoumianakis^a, Alison C. Brewer^d, Rana Sayeed^c, George Krasopoulos^c, Mario Petrou^c, Akansha Tarun^a, Dimitris Tousoulis^c, Ajay M. Shah^d, Barbara Casadei^a, Keith M. Channon^a, Charalambos Antoniades^a

^aDivision of Cardiovascular Medicine, Radcliffe Department of Medicine, University of Oxford, United Kingdom

^bCardiac Electrophysiology Group, Department of Physiology, Maastricht University, Netherlands

^cDepartment of Cardiology, Athens University Medical School, Athens, Greece

^dCardiovascular Division, King's College London BHF Centre, London, United Kingdom

^eDepartment of Cardiac Surgery, John Radcliffe Hospital, Oxford United Kingdom

1st Author's Surname: Antonopoulos

Short title: Epicardial adipose tissue and myocardial redox

Corresponding author

Charalambos Antoniades MD PhD

Associate Professor of Cardiovascular Medicine

Division of Cardiovascular Medicine, University of Oxford

John Radcliffe Hospital, Oxford OX3 9DU, United Kingdom

Tel: +44-1865-228340, Fax: +44-1865-740352

e-mail: antoniad@well.ox.ac.uk

Detailed Methods

Blood Sampling and Circulating Biomarkers Measurements

Venous blood samples were obtained after 8 hours of fasting, at the morning of the operation for measurements of circulating biomarkers. After centrifugation at 2000 g / 4°C for 15 min, plasma or serum was collected and stored at -80 °C until assayed. Whole blood was also collected for genotyping. Serum adiponectin and interleukin 6 (IL-6), a marker of inflammation, were measured using enzyme linked immunosorbent assays (ELISA) (BioVendor, Brno, Czech Republic and R&D systems USA respectively). Plasma malonyldialdehyde (MDA), a marker of systemic oxidative stress, was quantified by using the TBARS fluorometric assay, as previously described.¹ High sensitivity C-reactive protein (hsCRP), another marker of inflammation, was measured by the high-sensitivity latex enhanced immunoturbidimetric assay (ADVIA, Bayer HealthCare LLC). Plasma BNP was quantified by chemiluminescent-microparticle immunoassay (Architect BNP, Abbott, Germany).

DNA Extraction and Genotyping

Genomic DNA was extracted from whole blood using standard methods (QIAamp DNA blood Midi kit, Qiagen). Genotyping for the rs17366568 (functional polymorphism in *ADIPOQ* gene) and rs266717 SNPs (functional polymorphism in *ADIPOQ* gene promoter) was performed using TaqMan probes (Applied Biosystems; Assay IDs: C-33187752-10 and C-8288442-10 respectively). The assay was run on an ABI StepOne Plus PCR system according to the manufacturer's protocol.

Harvesting of Human Myocardium and Adipose Tissue Samples

During CABG, myocardial tissue samples were collected from the site of right atrial appendage (RAA) as we have previously described, and transferred into oxygenated (95% O₂ / 5% CO₂) ice-cold buffer. Samples of EpAT were harvested from the site of the right atrioventricular groove (inside the pericardial sac, attached to the heart), while thoracic adipose tissue (ThAT) samples were harvested from outside the pericardium (as "control" samples to the EpAT) and transferred in ice-cold phosphate buffer saline. All tissue samples were transferred immediately to the lab and either used for *ex-vivo* experiments or stored at -80°C for other studies as described below.

Myocardial Superoxide Measurements

Myocardial O₂⁻ production was measured in samples of right atrium appendages using lucigenin (5µmol/L)-enhanced chemiluminescence, as we have previously described.¹ Myocardial tissue was homogenised in ice-cold Krebs HEPES Buffer pH 7.35 in the presence of protease inhibitor (Roche Applied Science, Indianapolis, IN) using a pre-cooled Polytron homogeniser. The contribution of NADPH oxidase activity to myocardial O₂⁻ production was quantified in the presence of NADPH 100µmol/L. The use of homogenates allows us to overcome issues regarding penetration of NADPH (which is a polar molecule) into the cells or tissue. In certain *ex vivo* experiments with myocardial tissue, Vas2870 (40 µmol/L, a specific pan NADPH oxidase inhibitor²) was also used to get the Vas2870-inhibitable O₂⁻ signal as a more specific index of NADPH oxidase activity. In a pilot experiment comprising 10 RAA samples, we found that VAS2870 inhibitable O₂⁻ (pan-Nox inhibitor) was co-linear to the gp91dstat-inhibitable O₂⁻ (specific for Nox2) with r=0.8875 and P=0.0012. Therefore the use of vas2870 as an NADPH-oxidase inhibitor in the human right atrial appendage provides information mainly on Nox2-derived O₂⁻.

DHE Staining Method

In situ O₂⁻ production was determined in right atrial appendage cryosections with the oxidative fluorescent dye dihydroethidium (DHE) as previously described.^{3,4} Briefly, myocardial tissue was washed in ice-cold Krebs HEPES buffer and then cut into thin strips containing all myocardial layers. The tissue was first equilibrated for 20min in Krebs HEPES Buffer pH 7.35 at 37°C and then incubated for 2 hours in the presence or absence of recombinant full-length adiponectin 0.3 µmol/L (10 µg/ml, BioVendor) +/- CC (10 µmol/L). At the end of the incubation period tissue was collected and snap frozen in OCT. Myocardial cryosections (30µm) were equilibrated in Krebs Hepes buffer with or without Vas2870 (40µmol/L) or peg-SOD (300 U/ml). Then the samples were incubated with DHE (2µmol/L for 5 minutes). Fluorescence images of the myocardium (x63, Zeiss LSM 510 META

laser scanning confocal microscope) were obtained from each myocardial tissue quadrant. In each case, segments of myocardial tissue (with and without Vas2870 or peg-SOD) were analyzed in parallel with identical imaging parameters. DHE fluorescence was quantified by using Image-Pro Plus software (Media Cybernetics), while all analyses were performed in a blinded fashion.

RNA Isolation and Quantitative Real Time-Polymerase Chain Reaction (qRT-PCR) Samples of adipose tissue and myocardial tissue samples were snap frozen in QIAzol (Qiagen, Stanford, CA) and stored at -80°C until processed. RNA was extracted by using the RNeasy Micro or Mini kit (Qiagen). RNA was converted into complementary DNA (Quantitect Rev. Transcription kit - Qiagen), then subjected to qPCR using TaqMan probes (Applied Biosystems, Foster City, CA). The reactions were performed in triplicate in 384-well plates, using 5 ng of cDNA per reaction, on an ABI 7900HT Fast Real-Time PCR System (Applied Biosystems). The efficiency of the reaction in each plate was determined based on the slope of the standard curve; relative expression of *ADIPOQ* gene was calculated using the Pfaffl method ⁵.

For the clinical studies, *PPIA* (cyclophilin) and *PGK1* were used as housekeeping genes for adipose tissue and myocardial tissue, respectively. The Assay IDs of the Taqman probes used were *ADIPOQ* (adiponectin gene): Hs00605917_m1; *ADIPOR1*: Hs01114951_m1, *ADIPOR2*: Hs00226105_m1, *CDH13*: Hs01004530_m1, *CD36*: Hs01567185_m1, *PPARG*: Hs01115513_m1, *PGK1*: Hs00943178_g1, *PPIA*: Hs04194521_s1, *CYBB(NOX2)*, *NOX4*, *CYBA (P22PHOX)*, *NCF1 (P47PHOX)*, *NCF2(P67PHOX)*.

For the rat epicardial adipose tissue (see below), *PPIA* was used as housekeeping gene. The Assay IDs of the Taqman probes used were *PPIA*: Rn00690933_m1, *ADIPOQ*: Rn00595250_m1, *PPARG*: Rn00440945_m1, *CD36*: Rn00560963_s1.

For the mouse model (see below), *PPIA* and actin-alpha (*ACTA*) were used as housekeeping genes for adipose tissue and myocardial tissue, respectively. The Assay IDs of the Taqman probes used were *ACTA*: Mm00808218_g1, *ADIPOQ*: Mm00456425_m1, *ADIPOR1*: Mm01291334_mH, *ADIPOR2*: Mm01184032_m1, *CDH13*: Mm00490584_m1, *PPIA*: Mm02342429_g1.

For the pig model, *PPIA* and actin-beta (*ACTB*) were used as housekeeping genes for adipose tissue and myocardial tissue, respectively. The assay IDs of the Taqman probes used were *ACTB*: Ss03376160_u1, *ADIPOQ*: Ss03384375_u1, *ADIPOR1*: Ss03378803_u1, *ADIPOR2*: Ss03391825_g1, *CDH13*: Ss03386756_u1, *PPIA*: Ss03394782_g1.

Western Blots in human myocardial samples

To investigate adiponectin-AMPK signaling axis and its effects on NADPH oxidase activity, western immunoblotting was used to examine the direct effects of adiponectin on phospho(Th172)-AMPK α , total AMPK α , phospho(Ser473)-Akt, pan-Akt, phospho(Ser79)-acetyl-CoA carboxylase (ACC) and total ACC (antibodies by Cell Signaling, Danvers, MA), Nox1, Nox2 (antibodies by BD Transduction Laboratories), Nox4, Nox5 (antibodies by Abcam, Cambridge, UK), phospho(Ser359)-p47phox, total p47phox, p67phox (antibodies by Cell Signaling), and total Rac1 (antibody by Merck Millipore, Billerica, MA) protein levels in human myocardium incubated *ex-vivo*. Selected myocardial tissue samples from Clinical Associations Studies were also used to evaluate the content of 4-hydroxynonenal (4HNE) and malonyldialdehyde (MDA) adducts, the two most common lipid oxidation products (formed when reactive oxygen species react with lipid membranes, antibodies by Abcam) in the presence of high or low myocardial NADPH-stimulated O₂⁻ generation. Briefly, myocardial tissue samples were homogenized for 30 seconds using a pre-cooled electric Polytron homogenizer in 300 μ l of lysis buffer (Invitrogen, UK) containing a protease and phosphatase inhibitor cocktail (Roche Applied Science). Homogenates were spun at 13,000 rpm for 10 minutes, at 4 °C. The protein concentration of the supernatants was then measured using the BCATM Protein Assay kit (Pierce, UK). Protein lysates were separated on 4-12% gradient SDS-NuPAGE gel (Invitrogen, UK), and proteins transferred to polyvinylidene difluoride membranes (Amersham, UK Ltd.), followed by blocking with 5% powdered skimmed milk. The membranes were incubated with the respective primary antibodies overnight and immunodetection of the primary antibodies was performed with horseradish-peroxidase-conjugated secondary antibodies (Promega) and enhanced chemifluorescence (Amersham Bioscience UK Ltd.) and quantified in relation to the house-keeping protein, GAPDH (Santa Cruz Biotechnology, Santa Cruz, CA).

Measurement of Myocardial Rac1 Activation and Membrane Translocation Experiments

Rac1 activation was evaluated by a commercially available affinity precipitation assay using the PAK1-PBD conjugated glutathione agarose beads (Millipore, Temecula, USA)³. To estimate membrane translocation of Rac1 and p47phox, we performed differential centrifugation for isolation of membrane proteins, and membrane-translocated Rac-1 and p47phox proteins were determined by Western immunoblotting as previously described.³

Measurement of intracellular NADP/NADPH levels

For measurements of intracellular NADP/NADPH levels, a commercially available fluorometric assay was used (Abcam kit, Cambridge, UK). Following the 18 hour treatment, H9C2 cells were washed 3x with PBS and then lysed. Twenty five μ l of the lysates were loaded into a black walled 96-well plate for processing. Finally, 75 μ l of NADPH reaction mixture was added to initiate the reaction according to manufacturer's instructions and after 45 minutes the fluorescence was measured at Ex/Em=540/590nm. The assay kit provides measurements of intracellular NADPH, NADP and total NADPH/NADP separately.

Animal studies

Generating the mouse model: The cardiomyocyte-specific *NOX2* overexpressing mouse model (*mNOX2-tg*) was generated in the laboratory of Ajay Shah.⁶ The expression of the human 1.8kb *NOX2* cDNA was driven by the mouse myosin light chain-2 (MLC-2v) promoter. Transgenic founders were backcrossed for >10 generations onto a C57BL/6 background.

The decision to overexpress human *NOX2* in these mice was based on our findings in Clinical Associations Studies in which *NOX2* gene expression was strongly correlated with myocardial $O_2^{\cdot-}$ in the human right atrium appendages (Online Figure X), while its activation depends on p47^{phox} phosphorylation/membrane translocation and Rac1 activation. On the other hand, unlike Nox2, Nox4 does not require Rac1/p47phox membrane translocation to be activated, and exploring its role in this setting was beyond the scope of the current study.

Pig model: In 10 Dutch Landrace pigs (62 \pm 3 kg), anesthesia was induced with Zoletil (5-8mg/kg i.m.) and Thiopental (5-15mg/kg i.v.). After intubation, anesthesia was maintained by intravenous infusion of Midazolam (1.0mg/kg/h), Sufentanyl (4mg/kg/h) and Propofol (2.5-10mg/kg/h). An endocardial lead (Capsurefix 5568, Medtronic, Minneapolis, MN) was implanted in the right atrium and connected to a subcutaneous pacemaker (Itrel II, Medtronic, Minneapolis, MN). Healthy pigs (61 \pm 2 kg) served as a control group. After one week recovery, the pacemaker was switched on at a rate of 10Hz for 5 weeks. The ventricular rate was controlled by digoxin 10 μ g/kg for 1 week, followed by 5 μ g/kg for 4 weeks. Digoxin was discontinued 3 days before the sacrifice experiment in order to reach plasma levels <0.5 μ g/ml. At sacrifice, animals were anesthetized as described above and the heart was excised via a left lateral incision. Epicardial adipose tissue was collected from the posterior left atrium, close to the AV ring. For comparison, subcutaneous fat was taken from the incision in the thorax.

Power calculations

Sample size calculations were based on previous data from our laboratory. For the clinical studies, we estimated that a total number of 200 subjects would allow us to detect a 0.31 (or 7.5%) difference in log(myocardial NADPH-stimulated $O_2^{\cdot-}$) between the extreme tertiles of plasma adiponectin with an $\alpha=0.05$, a power of 0.9, and an assumed standard deviation of 0.57. For the ex vivo experiments, sample size calculations were performed on the basis of pilot experiments and we estimated that with a minimum of 5 pairs of samples (serial samples from the same myocardial tissue), we would be able to identify a change in log(myocardial NADPH-stimulated $O_2^{\cdot-}$) of 0.84 (or 20%) with an $\alpha=0.05$, a power 0.9, and a standard deviation for a difference in the response of the pairs of 0.44. Power calculations for the animal experiments were based on pilot data on adiponectin expression from epicardial adipose tissue; for the transgenic mice experiments, we estimated that with a minimum of 5 mice per group, we would be able to identify a change in adiponectin gene expression of 0.51 (2fold change) with an $\alpha=0.05$, a power 0.9, and a standard deviation for a difference in the response of the pairs of 0.22. Similarly, for the pig model of atrial pacing, we estimated that with a minimum of 5

pigs per group, we would be able to identify a change in adiponectin gene expression from epicardial adipose tissue of 0.91 (3fold change) with an $\alpha=0.05$, a power 0.9, and a standard deviation for a difference in the response of the pairs of 0.39.

Supplemental Tables

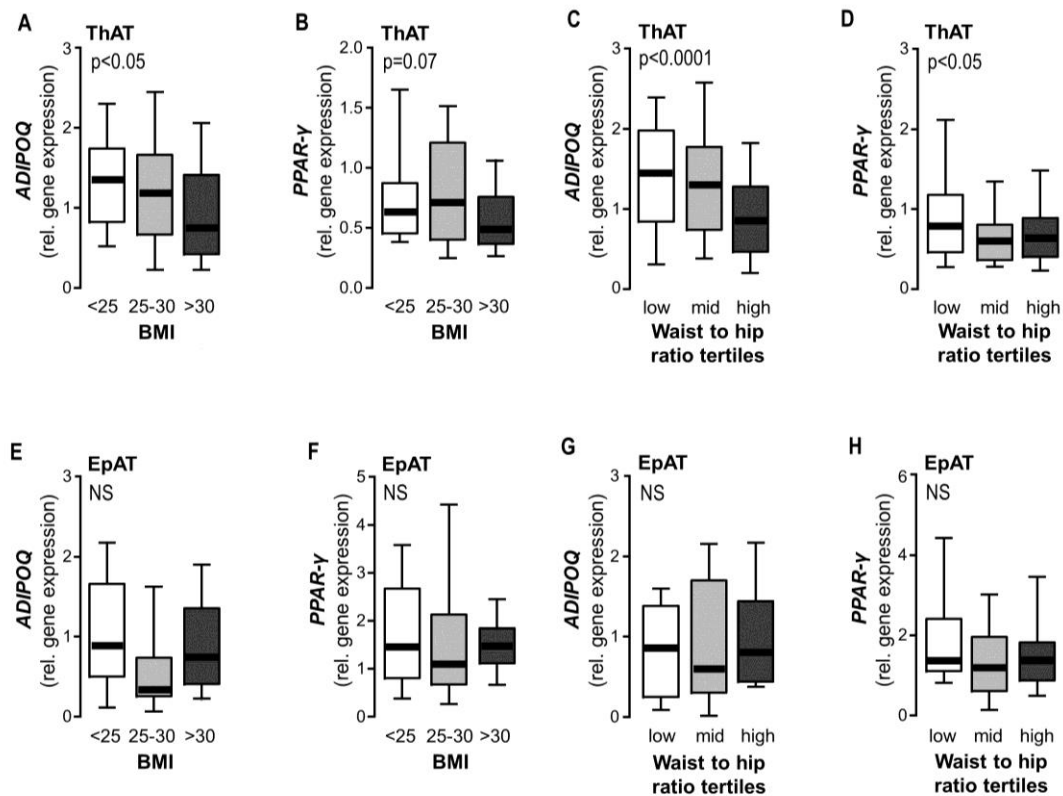
Online Table I: Multivariable models of myocardial NADPH-stimulated O_2^- and serum adiponectin

Model for myocardial NADPH-stimulated O_2^-		
Univariate analysis		
<i>Variable</i>	<i>Correlation coefficient*</i>	<i>P-value</i>
Log(serum adiponectin)	0.361	0.0001
Log(plasma BNP)	-0.045	0.601
Age	0.179	0.031
Male gender	-0.220	0.007
Smoking status	0.153	0.064
Left ventricular ejection fraction	-0.213	0.023
Multivariable analysis (R^2 for the model: 0.211, $P=0.001$)		
<i>Variable</i>	<i>Standardized beta</i>	<i>P-value</i>
Log(serum adiponectin)	3.802	0.001
Log(plasma BNP)	-0.08	0.465
Age	0.063	0.526
Male gender	-0.086	0.419
Smoking status	0.034	0.734
Left ventricular ejection fraction	-0.163	0.137
Model for circulating adiponectin		
Univariate analysis		
<i>Variable</i>	<i>Correlation coefficient*</i>	<i>P-value</i>
Log(NADPH stimulated O_2^-)	0.361	0.0001
Log(plasma BNP)	0.257	0.0001
Male gender	-0.175	0.008
Age	0.224	0.001
Body mass index	-0.126	0.07
Diabetes mellitus	-0.128	0.05
Hypercholesterolaemia	-0.175	0.009
Multivariable analysis (R^2 for the model: 0.215, $P=0.0001$)		
<i>Variable</i>	<i>Standardized beta</i>	<i>P-value</i>
Log(NADPH stimulated O_2^-)	0.210	0.016
Log(plasma BNP)	0.229	0.008
Male gender	-0.210	0.017
Age	-0.042	0.082
Body mass index	-0.148	0.225
Diabetes mellitus	-0.067	0.423
Hypercholesterolaemia	-0.102	0.628

BNP: Brain natriuretic peptide; *Spearman's or Pearson's correlation coefficient as appropriate

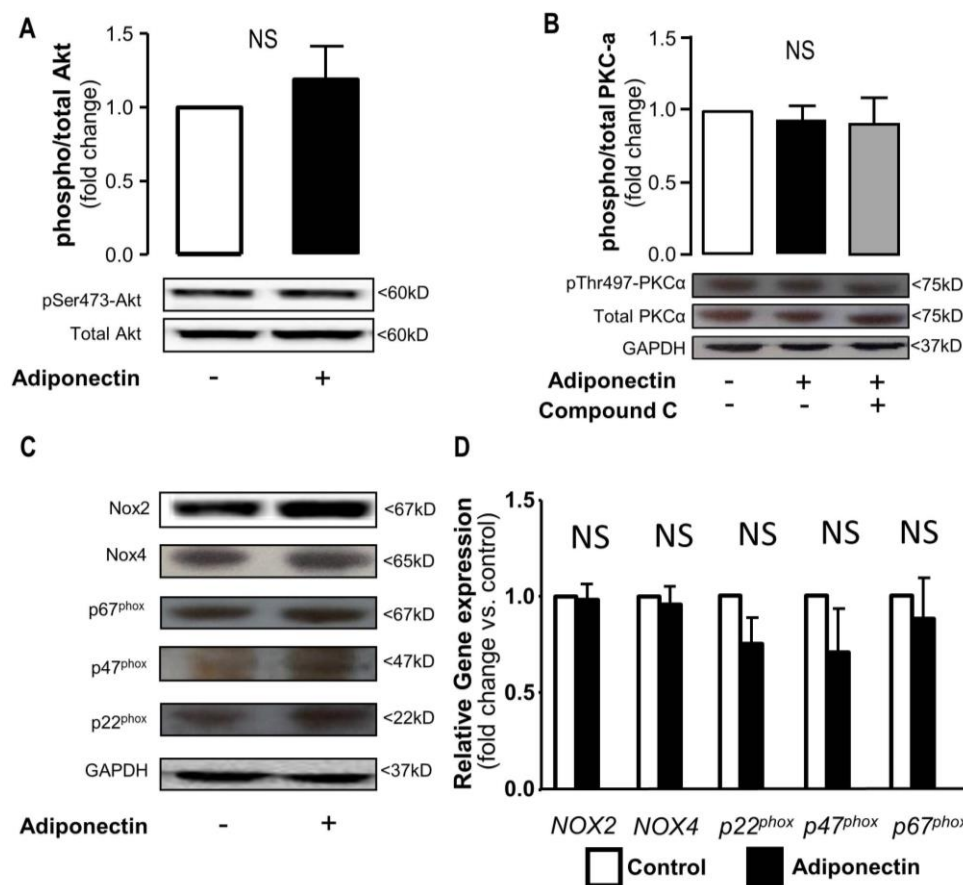
Supplemental Figures and Figure Legends

Online Figure I



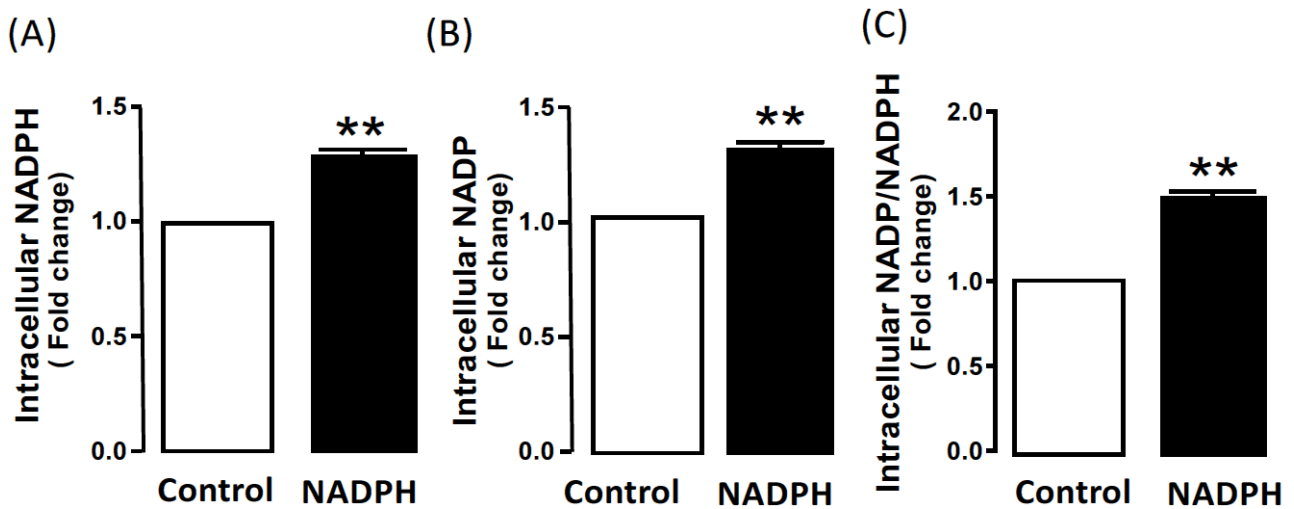
Obesity and adiponectin/PPAR- γ gene expression in thoracic and epicardial adipose tissue. In patients of Clinical Associations Studies (clinical cohort of 247 patients undergoing coronary artery bypass grafting), there was a significant inverse association between increased body mass index (BMI) and adiponectin gene (*ADIPOQ*) expression from thoracic adipose tissue (AT, Panel A). A trend towards lower PPAR- γ gene expression from thoracic AT with increased BMI was observed too but this did not reach statistical significance (Panel B). Abdominal obesity as assessed by the waist to hip ratio was also associated with lower *ADIPOQ* (Panel C) and *PPAR-γ* gene expression (Panel D) from thoracic AT. On the other hand, BMI and waist to hip ratio were not associated with adiponectin (Panel E & G) or *PPAR-γ* gene expression (Panel F & H) in epicardial AT. p-values are derived from ANOVA.

Online Figure II



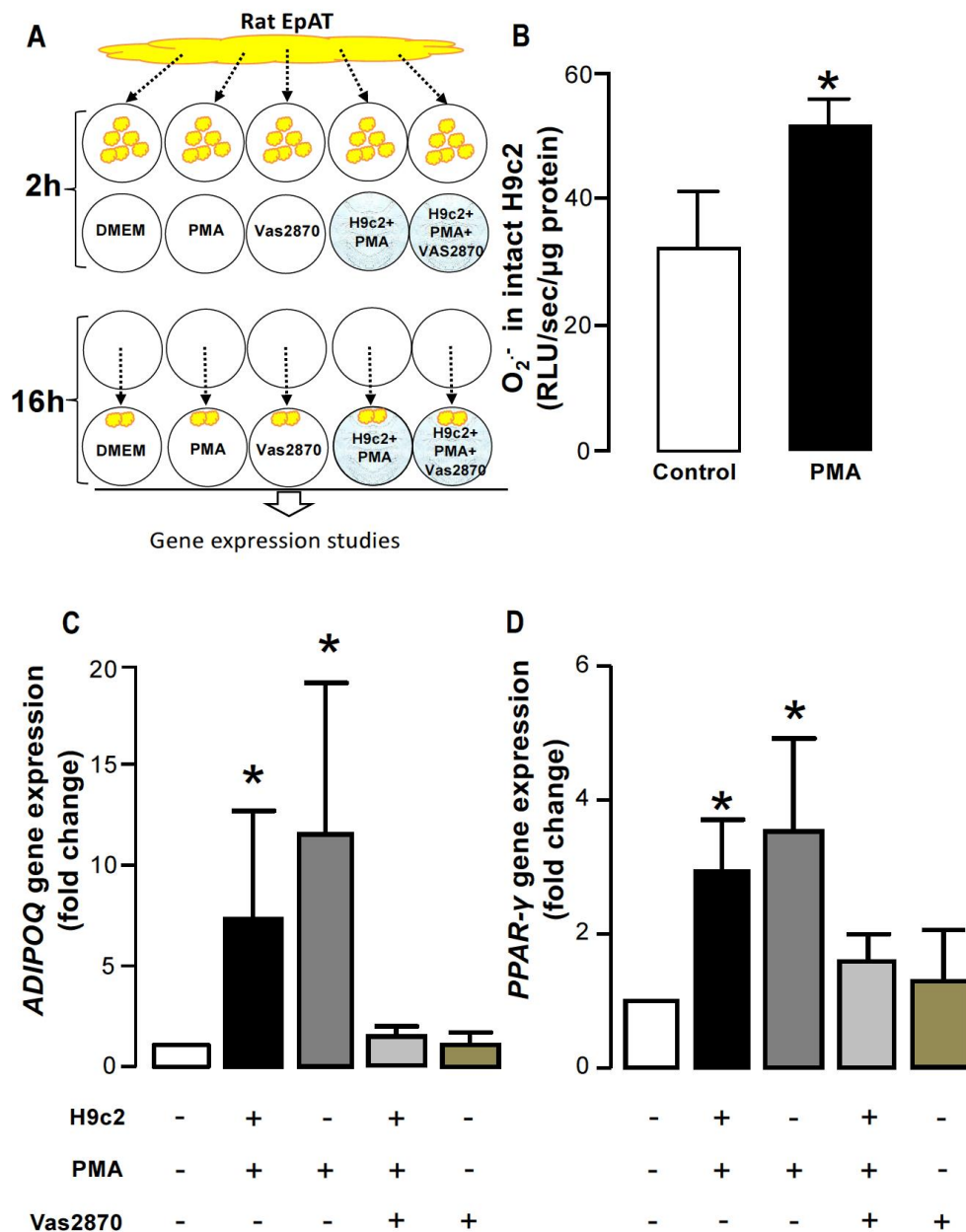
Effects of recombinant adiponectin on the expression of NADPH oxidase subunits and protein kinase C-α phosphorylation. Human myocardium was incubated ex-vivo for 2h in the presence or absence of recombinant human adiponectin (10μg/mL). Adiponectin did not lead to a significant increase in activity of Akt in this tissue, as assessed by Western blotting for phospho-Ser473 Akt, even though a positive trend was observed (Panel A). There was also no effect of adiponectin on the phosphorylation of protein kinase C-α at Thr497 (PKCα, Panel B), suggesting that its effects on NADPH oxidase were independent of any effects on Akt or PKCα signalling. Moreover, adiponectin did not have any effects on the protein levels of Nox2 and Nox4 isoforms or the protein levels of NADPH oxidase subunits, namely p22^{phox}, p47^{phox} and p67^{phox} (Panel C-D). n=10-12 for the adiponectin group and n=5-7 for the compound C; NS vs control group.

Online Figure III



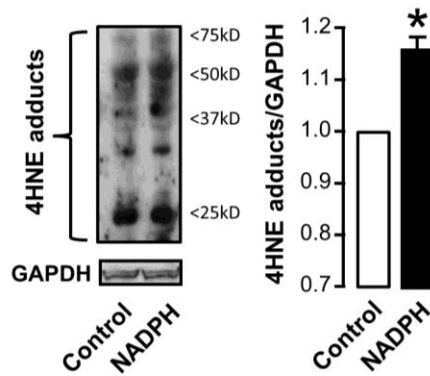
Changes of intracellular NADP/NADPH levels after incubation with exogenous NADPH. H9C2 cells were incubated with / without NADPH 100 μ mol/L for 18h, in conditions that mimic the co-culture experiments. Then the cells were washed thoroughly and lysed to measure intracellular concentration of NADPH, NADP and total NADP/NADPH using a fluorometric assay. There was a significant increase of both NADPH (by ~25%, A) and NADP (by ~25%, B), with the total NADP/NADPH being increased by ~45% (C) compared to control (**P<0.001 vs control). N=6 independent experiments.

Online Figure IV



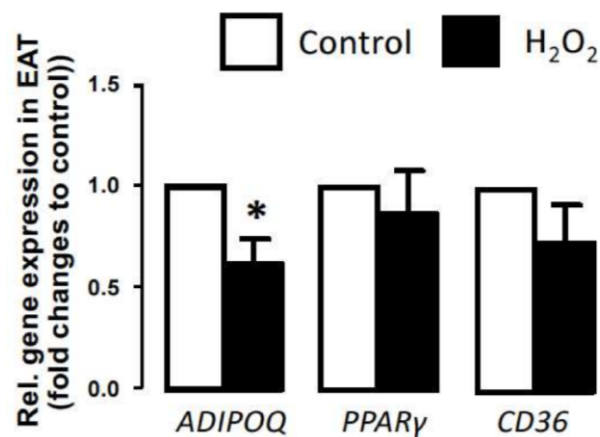
Co-culture of rat epicardial adipose tissue and H9C2 cells pre-stimulated with PMA. To examine whether under conditions of increased endogenous oxidative stress cardiomyocytes release a transferable factor able to affect the activation of PPAR- γ /adiponectin signalling in rat epicardial adipose tissue (EpAT), we exposed H9c2 cells to Phorbol-12-Myristate-13-Acetate (PMA, 160 nmol/L) while rat EpAT was conditioned *ex vivo* (Panel A). After 2h, the rat EpAT was transferred into the H9c2 wells and co-cultured for an additional 16 hours (Panel A). At the end of the incubation period, gene expression of PPAR- γ and ADIPOQ were studied in the rat EpAT. Addition of PMA to intact H9c2 cells grown on coverslips led to a striking increase of NADPH oxidases-derived superoxide ($O_2^{\cdot -}$, Panel B), as demonstrated by real-time monitoring using lucigenin-enhanced chemiluminescence. Co-incubation of rat EpAT with H9c2 cardiomyocytes stimulated with PMA resulted in an up-regulation of ADIPOQ (Panel C) and PPAR- γ expression (Panel D) in EpAT at 16h. These effects were prevented by VAS2870 (10nmol/L). However, PMA alone had a similar direct effect on ADIPOQ and PPAR- γ expression in EpAT even in the absence of H9C2 cells. DMEM: Dulbecco's Modified Eagle Medium; n=7 independent experiments; *p<0.05 vs control group.

Online Figure V



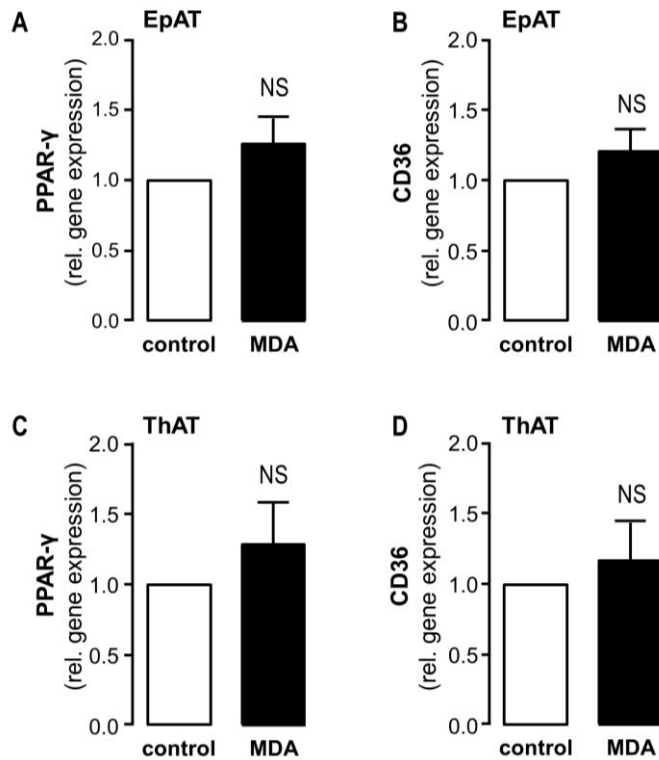
Short-term NADPH stimulation of human myocardium increases the formation of 4-HNE adducts. Human myocardium from patients undergoing coronary artery bypass grafting operation was incubated ex vivo for 16h +/- NADPH 100μmol/L (as a means to induce superoxide generation from NADPH oxidase). This interaction resulted in increased formation of 4-hydroxynonenal protein adducts (by-products of lipid oxidation) in myocardial tissue (Panel A). n=5 independent experiments; *p<0.05 vs control group.

Online Figure VI



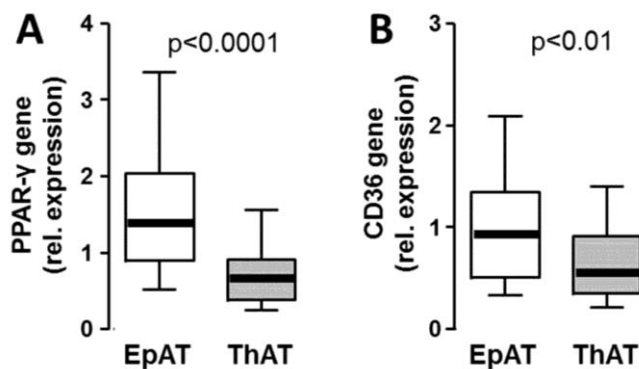
Ex vivo incubations of human epicardial adipose tissue with H₂O₂. Exposure of human epicardial adipose tissue (EAT) to H₂O₂ (100 μmol/L) for 16 h led to a significant reduction in adiponectin (*ADIPOQ*) gene expression, with no significant changes in *PPARγ* or *CD36* expression (n=8 independent experiments, *p<0.05 vs control).

Online Figure VII

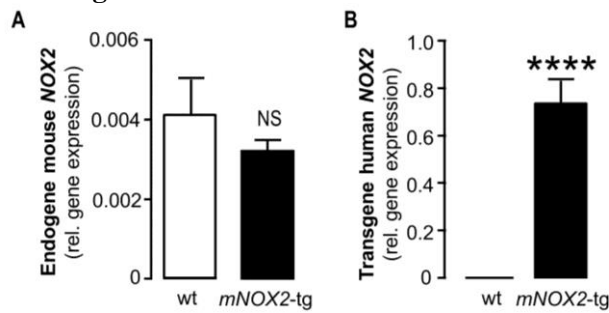


Ex-vivo incubation of epicardial (EpAT) and thoracic (ThAT) adipose tissue with malonyldialdehyde (MDA). EpAT and ThAT from 6 patients undergoing coronary artery bypass grafting was incubated ex-vivo for 16 hours in the presence or absence of MDA 1mM and used for gene expression studies. MDA did not have any effects on the relative expression levels of PPAR- γ and CD36 gene in either EpAT (Panels A-B) or ThAT (Panels C-D). n=5-6 independent experiments; NS: non significant vs control group.

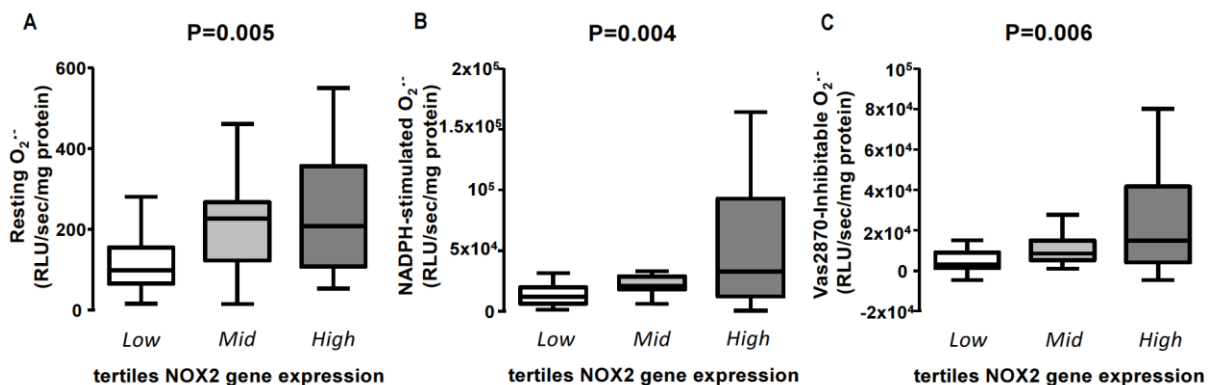
Online Figure VIII



Comparison of peroxisome proliferator activated receptor- γ (PPAR- γ) expression and activation between human adipose tissue depots. Adipose tissue samples of patients with coronary artery disease, were used to compare the expression of PPAR- γ and its downstream mediator CD36 in epicardial (EpAT) vs thoracic adipose tissue (ThAT). Both the expression of PPAR- γ (A) and its downstream molecule CD36 (B) were higher in EpAT compared to ThAT.

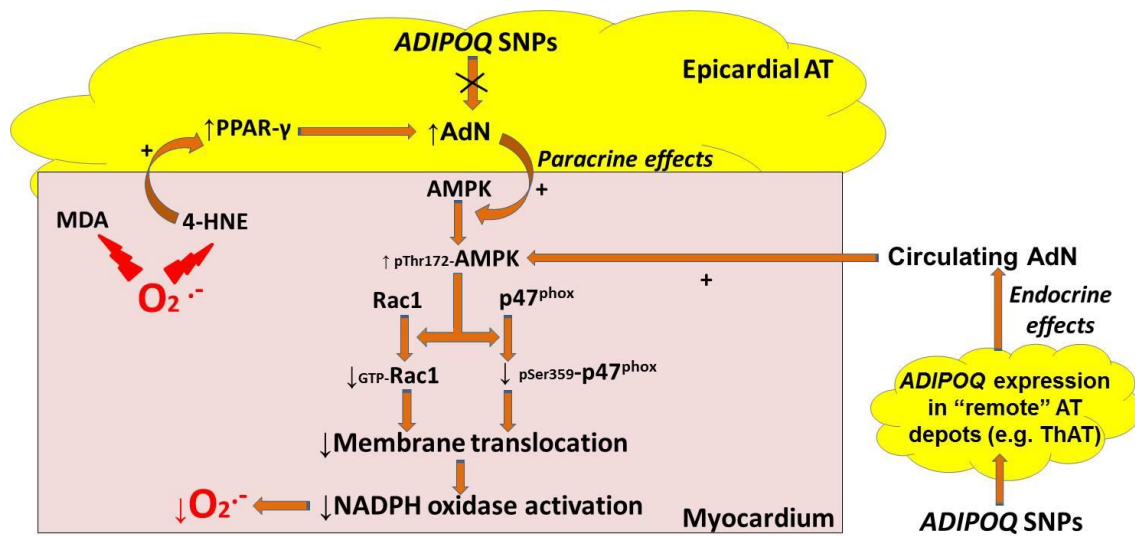
Online Figure IX

Mouse model of cardiomyocyte-specific overexpression of human *NOX2*. There was no difference in the expression of murine *NOX2* in the heart of *mNOX2-tg* vs the wild type (wt) animals (Panel A). On the contrary, *mNOX2-tg* mice were over-expressing human *NOX2* in their cardiomyocytes, which was not expressed in the wt mice (Panel B). n=9-10 per group; NS: non-significant; ****p<0.0001 vs wt.

Online Figure X

***NOX2* expression and $O_2^{\cdot-}$ generation in the human right atrium appendages (RAA).** High *NOX2* gene expression in human RAA was significantly associated with increased resting $O_2^{\cdot-}$ (A), NADPH-stimulated $O_2^{\cdot-}$ (B) and Vas2870-inhibitable $O_2^{\cdot-}$ (C) in the same tissue.

Online Figure XI



Schematic representation of the bi-directional signalling between epicardial adipose tissue and the myocardium. The cross-talk between epicardial adipose tissue (EpAT) and the myocardium involves the release of oxidation products from the heart (4-hydroxynonenal- 4HNE) able to trigger peroxisome proliferator activated receptor (PPAR)- γ – induced expression of adiponectin (AdN) in EpAT, which may suppress NADPH oxidases activity in the underlying heart muscle in a paracrine way, via an AMPK (AMP kinase) –dependent activation of Rac1 and phosphorylation of p47^{phox} subunits of NADPH oxidase. AT: Adipose Tissue.

Supplemental References

1. Antoniadou C, Demosthenous M, Reilly S, Margaritis M, Zhang MH, Antonopoulos A, Marinou K, Nahar K, Jayaram R, Tousoulis D, Bakogiannis C, Sayeed R, Triantafyllou C, Koumallos N, Psarros C, Miliou A, Stefanadis C, Channon KM and Casadei B. Myocardial redox state predicts in-hospital clinical outcome after cardiac surgery effects of short-term pre-operative statin treatment. *J Am Coll Cardiol*. 2012;59:60-70.
2. Wingler K, Altenhoefer SA, Kleikers PW, Radermacher KA, Kleinschnitz C and Schmidt HH. VAS2870 is a pan-NADPH oxidase inhibitor. *Cell Mol Life Sci*. 2012;69:3159-60.
3. Antoniadou C, Bakogiannis C, Tousoulis D, Reilly S, Zhang MH, Paschalis A, Antonopoulos AS, Demosthenous M, Miliou A, Psarros C, Marinou K, Sfyras N, Economopoulos G, Casadei B, Channon KM and Stefanadis C. Preoperative atorvastatin treatment in CABG patients rapidly improves vein graft redox state by inhibition of Rac1 and NADPH-oxidase activity. *Circulation*. 2010;122:S66-73.
4. Kim YM, Guzik TJ, Zhang YH, Zhang MH, Kattach H, Ratnatunga C, Pillai R, Channon KM and Casadei B. A myocardial Nox2 containing NAD(P)H oxidase contributes to oxidative stress in human atrial fibrillation. *Circ Res*. 2005;97:629-36.
5. Pfaffl MW. A new mathematical model for relative quantification in real-time RT-PCR. *Nucleic Acids Res*. 2001;29:e45.
6. Brewer AC, Murray TV, Arno M, Zhang M, Anilkumar NP, Mann GE and Shah AM. Nox4 regulates Nrf2 and glutathione redox in cardiomyocytes in vivo. *Free Radic Biol Med*. 2011;51:205-15.